Enzymatic Modification of Oat Proteins for Barista Oat Drinks

Amala Theresa George

DIVISION OF FOOD AND PHARMA | DEPARTMENT OF PROCESS AND LIFE SCIENCE ENGINEERING FACULTY OF ENGINEERING LTH | LUND UNIVERSITY

2026

MASTER THESIS

Enzymatic Modification of Oat Proteins for Barista Oat Drinks

Linking Structure to Foaming and Coffee Stability

Amala Theresa George

Enzymatic Modification of Oat Proteins for Barista Oat Drinks

Linking Structure to Foaming and Coffee Stability

Published by
Department of Process and Life Science Engineering
Faculty of Engineering LTH, Lund University
P.O. Box 118, SE-221 00 Lund, Sweden

Subject: KLTM02 Degree Project in Food Engineering, Nutrition and Food Chemistry

Division: Food and Pharma
Supervisor: Anna Fureby
Examiner: Lars Nilsson

Enzymatic Modification of Oat Proteins for Barista Oat Drinks

Linking Structure to Foaming and Coffee Stability

by

Amala Theresa George

Process and Life Science engineering

May 2026

Supervisor: Anna Fureby
Examiner: Lars Nilsson

Popular Science Summary

Enzymatic Craftsmanship: Reshaping Oat Proteins for the Perfect Coffee

Oat drink is sustainable, but in coffee applications it often fails due to the nature of its proteins. This project studies different enzyme treatments that reshape oat proteins to create a stable coffee with robust foam.

In recent times, global food systems have undergone a significant transition towards sustainability, with consumers increasingly choosing plant-based diets to reduce their environmental footprint. Among the coffee enthusiasts who are seeking a creamy, dairy-free alternative, oat drink has gained popularity. However, oat drink in a coffee cup presents a significant "Barista Challenge". Unlike cow's milk, proteins in oat drink have a rigid, tightly coiled structure. When introduced to the hot, acidic environment of a brewed coffee, these proteins react unfavourably causing them to clump together and curdle, while the foam collapses quickly.

The ability of a beverage to maintain a creamy, stable foam depends on the behaviour of proteins at the interfacial film which is the thin boundary between air and liquid. To function effectively, proteins must unfold and wrap around the air bubbles like a protective shield. However, the primary storage proteins in oat, known as 12S globulins, are too rigid to do this efficiently. To solve this issue, the food industry uses enzymes as molecular scissors to unfold the protein structure. This Master's thesis, conducted in collaboration with Cerealiq AB, sought to determine how different enzymatic treatments modify oat proteins to achieve barista-grade stability.

The study utilized a multi-analytical approach to look deeper into the molecular structure of the modified oat proteins. A key finding was that the precision of the enzymatic cut is as important as how much protein was cut and got dissolved. One treatment was highly efficient at extracting protein into the drink but created a polydisperse mixture. This system was much like trying to build a stable wall with bricks of random shape. The mismatched fragments could not pack together tightly, leading to a weak interfacial film that reduced the foam stability. In contrast, another specific treatment performed a limited proteolysis resulting in a more uniform less polydisperse population of protein fragments. These fragments arranged orderly and tightly around the bubbles to create a robust, viscoelastic film that kept the foam stable for more time.

Thus, the research shows that pairing a suitable protein modification enzyme technique with specific starch breaking enzymes, it is possible to develop a naturally creamy, stable oat drink suitable for coffee applications. These findings provide a scientific framework for engineering a sustainable, high-performance oat beverage.

Abstract

The rapid expansion of the plant-based beverage sector has increased the demand for high-performance, barista-grade oat drinks that are capable of withstanding the thermal and acidic stresses of coffee applications. This Master's thesis, conducted in collaboration with Cerealiq AB, evaluates the efficacy of six specific enzymatic treatments in modifying the structural and physical properties of oat protein to establish a rational structure-function relationship for enzyme selection. Using a multi-analytical approach, the study identified proteolytic control as the primary determinant of interfacial performance. Although Sample 1 (Protease 1) showed maximum protein solubility, its high molecular polydispersity hindered the formation of a cohesive interfacial film resulting in lower foam stability. In contrast, through limited proteolysis, Sample 5 and 6 (Protease 4) maintained molecular dispersity, facilitating an ordered molecular assembly at the air-water interface resulting in superior Foam Stability Index (FSI). Furthermore, the study confirmed that the maintenance of an appropriate particle size and apparent viscosity is essential for suppressing coalescence kinetics. Ultimately, this research provides a predictable framework for the enzymatic development of high-performance oat beverages for barista application by showing that superior foaming and colloidal stability depend on balancing protein solubility with molecular fragments which are less polydisperse and refined particle size.

Keywords: Oat protein, limited proteolysis, foam stability, colloidal stability, barista-grade

Acknowledgement

This Master's thesis was conducted in collaboration with Cerealiq AB in Bjuv. I would like to express my sincerest gratitude to everyone in the company especially Emilie Sellman, Angie Triantafyllou and Felix Mattsson for their support throughout this project.

I would also like to thank my supervisor, Anna Fureby for her guidance and for taking time to answer my questions. I also thank Lars Nilsson, Olexandr, Hans, Jesús Enrique and Andrius Jasilionis for their willingness for training me on the analytical methods.

Lastly, I would like to thank my family and friends for their support during this project and my studies.

Thank you,

Amala

Table of Contents

1. Introduction

1.1 Global Trends in Plant-Based Beverage Sector

In recent times, the global food systems are transitioning toward sustainability, with consumption pattern shifting significantly toward plant-based (PB) diets (Jaeger & Giacalone, 2021). This shift has fuelled a rapid expansion in the PB food market, particularly within the non-dairy PB beverage sector driven by increased health and environmental concerns, rising prevalence of lactose intolerance and flexitarian dietary patterns among consumers (Munekata et al., 2020). Consequently, the PB beverage market is projected to grow at a compound annual growth rate (CAGR) of 11.6% from 2024 to 2030 (De Santis et al., 2025). A diverse range of plant sources including cereals (rice, oats), nuts (almond, coconut), legumes (soy, pea), and seeds (flax, sunflower) are being utilized for the production of PB beverages (Rovai et al., 2025).

1.2 Characteristics and Comparative Advantages of Oat-Based Beverages

Out of all the available PB alternatives, oat drink has gained superior popularity due to its sensory appeal, nutritional profile and associated health benefits, and a low environmental footprint (Cui et al., 2024). Consumers value oat drink for its subtle sweetness, oaty and nutty flavour, and creamy texture which make it suitable for coffee applications (Rovai et al., 2025). Nutritionally, oat drink is characterized by proteins, unsaturated fatty acids, and β-glucans, which are associated with the prevention of cardiovascular diseases and type II diabetes (Bocchi et al., 2021). Furthermore, the presence of specific polyphenols such as avenanthramides, hydroxybenzoic acids, and hydroxycinnamic acids provide antioxidant properties (Soycan et al., 2019). Regarding ecological impact, oat drink production generates 62% to 78% fewer greenhouse gas emissions compared to dairy, while using less land and water (Ramsing et al., 2023).

1.3 Functional Challenges in Barista Applications

Despite this growing popularity, the performance of oat beverages in coffee applications is hindered by significant technical challenges, particularly in the creation and maintenance of stable foams. Foam is generated by the colloidal dispersion of air bubbles into the liquid phase by mechanical agitation, such as aeration or stirring (Sarkar and Singh, 2016; Zakidou et al., 2022). Surface-active proteins act as foaming agent to facilitate this process by adsorbing at the air-liquid interface to create an interfacial film, which delays bubble coalescence and slows the

drainage processes that lead to foam collapse (Hassan et al., 2024; Sarkar and Singh, 2016). However, unlike the flexible random-coil caseins found in bovine milk, the globular nature of the PB proteins inherently limits their interfacial functionality (Hassan et al., 2024). Besides, the repeated glutamine-rich regions on the oat protein surface reduces its hydrophilicity and results in poor water solubility. Furthermore, the relatively low protein content of oat drink (0.5 g/100g) compared to cow's milk (3.4 g/100g) constrains foam expansion and strength (Zakidou et al., 2022).

1.4 Colloidal Stability and Enzymatic Solutions

Beyond these structural limitations, the functional performance of oat proteins in barista applications also depends on the thermal and acidic conditions of coffee preparation. Globular oat proteins tend to denature, curdle, or aggregate when exposed to a temperature above 70°C thereby reducing both foamability and beverage stability (Hassan et al., 2024). Since the solubility of oat proteins is highly sensitive to the surrounding environment, the acidic pH of coffee, typically ranging between 4.5 to 6.0, often leads to emulsion breakdown (Mäkinen et al., 2024). To address these limitations, enzymatic modifications such as limited hydrolysis and deamidation are employed to improve the molecular flexibility of compact oat globulins and increase their net negative charge (Jiang et al., 2015; Mäkinen et al., 2024). These structural changes improve solubility and surface activity to facilitate the formation of stable interfacial films (Jiang et al., 2015).

1.5 Aim and Objectives

This master's thesis project is conducted in collaboration with Cerealiq AB, a provider of enzyme solutions for the PB beverage industry, to address the need for quantitative data in enzyme formulation. Establishing a clear structure-function relationship for application of enzymes in commercial production of barista-grade oat drink is essential for transitioning from trial-and-error method to a more predictable and rational approach to enzyme selection. To achieve this, the present study evaluates six specific enzyme combinations and characterizes how each treatment modifies the functional, physical, and surface properties of the oat protein. By analysing changes in certain parameters like particle size distribution, surface tension, and surface charge, this study seeks to determine how these enzyme-induced structural modifications affect the performance of oat drinks in coffee applications.

2. Theoretical Background

2.1 Oat Protein Biochemistry

2.1.1 Protein Composition

Cereal proteins are traditionally classified into four groups based on their solubility in different solvents, namely water-soluble albumins, salt-soluble globulins, alcohol-soluble prolamins (avenins), and dilute acid/alkali-soluble glutelins, a system known as the Osborne classification (McLauchlan et al., 2024). Unlike most other cereals in which prolamins are the dominant storage proteins, oats constitute a larger fraction of globulins, accounting for approximately 70-90% of the total protein (McLauchlan et al., 2024; Murakami et al., 2016). The remaining protein fraction is composed of about 4-14% prolamins (avenins), albumins at 1-12%, and glutelins, which generally account for less than 10% (Gil-González et al., 2024). Oat globulins are further characterized into 3S, 7S, and the most abundant 12S fractions based on their sedimentation coefficients (Mäkinen et al., 2024). The 12S globulin exists as a hexameric structure with a total molecular weight estimated between 322 to 330 kDa (Nnanna & Gupta, 1996; Peterson, 1978). This hexamer is composed of six subunits, each consisting of an acidic polypeptide (α; ~32-35 kDa) and a basic polypeptide (β; ~22 kDa) linked together by a disulfide bond (Peterson, 1978; Zhao et al., 2004). Research suggests that a significant portion of the residual protein remaining after salt extraction of oats consists of non-extracted 12S globulins that have aggregated or associated with other cell components (membrane, lipids, phenolics etc.) (Robert et al., 1985a, 1985b). Additionally, 12S globulin has compact molecular structure and a high denaturation temperature (110°C), which contributes to its poor solubility under the neutral and slightly acidic conditions common in food systems (McLauchlan et al., 2024).

2.1.2 Molecular Structure: Subunit Architecture and Interfacial Constraints

The quaternary architecture of the oat 12S globulin is an $(\alpha\beta)_6$ hexamer which consists of six monomeric units of approximately 54,000 Da. At the secondary structural level, the oat globulin is highly ordered. It comprises approximately 50% α-helical and 43% β-sheet structures, with a notably low proportion of disordered random coils (McLauchlan et al., 2024; Nnanna & Gupta, 1996). As discussed by Li & Xiong (2023), this organization gives a compact spheroid shape to the oat globulin in which the majority of non-polar (hydrophobic) groups are buried within the protein interior protected from the surrounding aqueous environment. This structure is stabilized by disulphide bonds that link the α and β polypeptides restricting molecular

flexibility and preventing conformational rearrangements required to expose the hydrophobic domains. Consequently, the native protein is thermodynamically limited from unfolding and adsorbing effectively at air-water or oil-water interface, which contributes to its poor functional performance and susceptibility to aggregate under destabilizing condition. Furthermore, the acidic α-polypeptide contains repeated octapeptides (Gln-Tyr-Gln-Glu/Val-Gly-Gln-Ser-Thr) near its C-terminus. These specific sequences have a neutral isoelectric point and are located on the surface of the globulin molecule where they are exposed to the solvent (Shotwell et al., 1988). The high level of internal disulfide bonding and neutral surface repeats results in a protein structure that is highly resistant to conformational rearrangements unless subjected to extreme pH shifts, enzymatic intervention, or the addition of chemical reducing agents (Li & Xiong, 2023; McLauchlan et al., 2024; Pynket et al., 2026).

2.1.3 Amino Acid Profile and Surface Hydrophilicity

Oat proteins have a relatively high proportion of essential amino acids, specifically lysine and threonine, which contributes to their superior nutritional quality compared to other major cereals (Klose & Arendt, 2012; Rafique et al., 2022). However, the storage fractions are dominated by glutamic acid (including glutamine) and proline, which together account for approximately 40-50% of the total amino acid content (Anderson, 2014). Amino acid analysis performed by Peterson (1978) indicated that the basic (β) polypeptide contains higher levels of glutamic acid/glutamine and glycine compared to the acidic (α) polypeptide, which is richer in basic amino acids and aspartic acid/asparagine. Additionally, the basic β–polypeptides are water soluble when separated from the acidic subunits and contain significantly higher levels of the essential amino acids, lysine and methionine (Nnanna & Gupta, 1996; Peterson & Brinegar, 1986). The α-polypeptide possesses a high density of glutamine residues within the surface-exposed octapeptide repeats, specifically in the Glo-23 sequence where glutamine accounts for 26 out of the 81 amino acids (Anderson, 2014). The oat repeats are largely uncharged compared to legume proteins like soy glycine where the surface regions are composed of charged acidic residues. The presence of these neutral amino acid clusters results in relatively hydrophobic surface which contributes to intermolecular association and reduced solubility, mainly near the isoelectric point and under thermal or acidic stress (Mäkinen et al., 2024; Shotwell et al., 1988; Wagner et al., 2000).

2.2 Enzymatic Modification Strategies

To overcome the inherent structural rigidity and poor solubility of native oat 12S globulins, enzymatic modification is employed to alter the protein's molecular architecture. These strategies focus on enhancing the surfactant properties required for stable foam formation and emulsion stability (McLauchlan et al., 2024).

2.2.1 Proteolysis

Enzymatic proteolysis is employed to improve the techno-functionality of oat protein by modifying its molecular size, conformation, and the strength of inter- and intra-molecular bonds (Ibrahim et al., 2022). During this process, enzymes catalyse the cleavage of peptide bonds which facilitates the unfolding of the complex globular structure. Specifically, the use of proteases such as Alcalase and trypsin promotes protein solubility by breaking down the 12S-oat globulin through peptide cleavage. While Alcalase primarily attacks glutamic acid residues, trypsin focuses on C-terminal arginine and lysine sites thereby disrupting the protein's globular arrangement leading to structural unfolding and varied molecular weight profiles (Brückner-Gühmann et al., 2021; Nieto-Nieto et al., 2014; Sánchez-Velázquez et al., 2021). Such limited proteolysis reduces the molecular weight of the globulin subunits preventing the formation of large, insoluble aggregates that occur when proteins are subjected to high temperatures (Brückner-Gühmann et al., 2021). Furthermore, as the primary structure is disrupted, buried hydrophobic parts are exposed to the solvent and eventually increase surface hydrophobicity to enhance the protein's affinity for the air-water interface. However, the extent of hydrolysis plays a crucial role as excessive exposure of hydrophobic patches may result in protein-protein association and aggregation. (Brückner-Gühmann et al., 2021; Ibrahim et al., 2022). When hydrolysis is limited, the exposure of hydrophobic regions is accompanied by an increase in conformational flexibility, solubility and in some cases net surface charge. All of this collectively favours interfacial adsorption and foaming, resulting in an overall shift towards improved functionality (Creusot & Gruppen, 2007; Ipsen et al., 2001).

2.2.2 Deamidation: Charge Enhancement

Protein deamidation using protein-glutaminase (PG) facilitates the conversion of amide side chains of glutamine residues into negatively charged glutamic acid (COO^-), releasing ammonia in the process (NH_3^+) (*Figure 2.1)* (Liu et al., 2022). Unlike traditional proteases, PG targets the surface charge of globular proteins and significantly increase the net negative charge without causing extensive disruption to the peptide backbone (Jiang et al., 2015). This

negatively charged glutamic acid increases the structural flexibility and hydration of the protein, doubling the water solubility of oat proteins compared to their native form (Immonen et al., 2021). Research by Immonen et al., (2022), indicates that this higher net charge also reduces the density of the interfacial layer due to increased repulsion between proteins, yet foamability is improved by dissociating high-order aggregates into smaller, more surface-active monomers.

Figure 2.1.: Schematic representation of enzymatic deamidation of protein bound glutamine to glutamic acid by protein-glutaminase (Liu et al., 2022).

2.2.3 Starch Hydrolysis

Starch is the predominant component of the oat kernel (40-65% w/w) characterized by a clustered granular architecture composed of semi-crystalline structures containing linear α-D-glucose amylose chains joined by α-1,4 bonds and highly polymerized amylopectin with extensive α-1,6 bonds (Jeong et al., 2022; Rostamabadi et al., 2022). Starch hydrolysis is the process of degrading this starch polymer through enzymatic deconstruction using α-amylase and glucoamylase. α-amylase is an endo-acting enzyme that randomly cleaves α-1,4-glucosidic bonds resulting in the viscosity reduction of the slurry during the initial liquefaction phase. Glucoamylase, on the other hand, acts as an exo-amylase and hydrolyse the non-reducing ends of starch to release glucose (Mendonça et al., 2023). Studies show that synergistic catalysis using amylases and debranching enzymes like pullulanase reduce the molecular weight of amylopectin and amylose, leading to improved emulsifying properties of the starch hydrolysates (Zhan et al., 2025).

2.3 Physical Chemistry of Food Colloids

2.3.1 Emulsions

Emulsions are formed when two immiscible fluids, mostly oil and water, are dispersed by forcing the system from a low energy state to a high energy state. They are thermodynamically unstable due to the high surface energy of the droplets and bubbles. To achieve kinetic stability, emulsifiers which are amphipathic molecules that adsorb at the oil/water interface are added to the system. This reduces the interfacial tension and creates a protective layer that prevents coalescence between the emulsion droplets (Langevin, 2025; Zafeiri et al., 2017). Proteins act

as effective emulsifiers due to their amphiphilic nature derived from the specific distribution of polar and non-polar amino acid residues. The process of protein adsorption to the oil-water interface mainly occurs in three distinct stages;

i. proteins migrate along a concentration gradient via convection and diffusion
ii. structural unfolding of the molecular chains to expose hydrophobic sites to the oil phase
iii. eventually forming a viscoelastic film (Zhang et al., 2022).

Proteins also exhibit a high free Gibbs energy which leads to slow desorption and for high-molecular mass proteins the adsorption process is effectively irreversible (Fainerman et al., 2005). Studies also suggests that increased conformational flexibility in globular proteins leads to higher rate of unfolding and faster adsorption at the interface (H. Zhang et al., 2022). Once adsorbed, the stability against coalescence is maintained by the formation of a cohesive viscoelastic film and the surface tension gradients known as Marangoni forces that slows down the thinning of films by resisting the motion of surfactant towards the film borders (Langevin, 2025).

2.3.2 Interfacial Adsorption: Kinetics and Conformational Rearrangement

The initial stage of protein adsorption involves the transport of molecules from the bulk aqueous phase towards the interface via biased diffusion. The structured water layers at the interface create an orientational ordering to effectively pull the peptides toward the surface from several angstroms away (Penna et al., 2014). The arrival rate of the protein at the interface is dependent on the bulk protein concentration and the diffusion coefficient of the protein (Yano et al., 2018). In dilute solutions, there is a characteristic lag phase where the interfacial tension remains unchanged over time as the diffusion rate of proteins to the interface is slow (Baldursdottir et al., 2010).

Once the proteins are adsorbed to the surface, they undergo structural rearrangement, often referred to as “surface-induced denaturation” (Hlady et al., 1999). The degree of initial deformation depends on the kinetics of adsorption. When the adsorption is slower than the unfolding rate, the protein can occupy a maximum interfacial area and achieve higher degree of unfolding (Yano et al., 2018). Following a stepwise and sequential adsorption of the residues, lockdown of the peptide on the surface occurs. This process is termed as statistical zippering (Penna et al., 2014). Due to the accelerated adsorption of the protein to the interface at this

stage, the interfacial tension drops. At the end, proteins adsorb to the surface as thin, monomolecular layer (Baldursdottir et al., 2010).

These molecular events are typically categorized by three distinct kinetic regimes observed in surface pressure-log time plots *(Figure 2.2.):*

i. Regime I: Dominated by diffusion and the protein's initial affinity for the interface (Beverung et al., 1999).
ii. Regime II: Characterized by a steep decline in surface tension as the protein molecules increase their contact points with the interface through unfolding (Baldursdottir et al., 2010; Beverung et al., 1999).
iii. Regime III: Occurs at the monolayer coverage, where the adsorbed layer undergoes continued relaxation with soft drop in interfacial tension, leading to multilayer build-up and formation of a viscoelastic gel-like network (Baldursdottir et al., 2010).

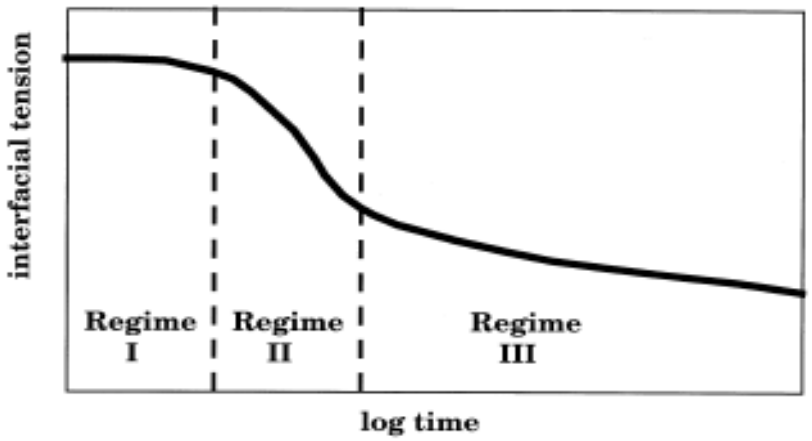

Figure 2.2.: Kinetic stages of interfacial tension reduction during protein adsorption. The curve represents the transition from the initial induction phase (I) to the active adsorption phase (II) and the final steady-state rearrangement phase (III) leading toward equilibrium surface tension (Beverung et al., 1999).

2.3.3 Stabilization Mechanisms

Colloidal stability in protein-stabilized systems is generally divided into two mechanisms; electrostatic stabilization, provided by the repulsive forces between similarly charged electrical double layers, and steric stabilization, which occurs when hydrophilic macromolecular chains are adsorbed onto the particle surface (Capek, 2002).

2.3.3.1 Electrostatic Stabilization and Zeta Potential

Electrostatic stabilization relies on the net surface charge of proteins to create a repulsive force that prevents aggregation. Jiang et al., (2015) explained that modifying oat proteins via deamidation introduces negatively charged carboxyl groups to the protein that increase this electronic repulsion enhancing water solubility and preventing precipitation in aqueous foods. This charge is quantified by the zeta potential and studies show that deamidated oat protein concentrates have been shown to exhibit significantly higher zeta potential (e.g., -50 mV) compared to native concentrates (Immonen et al., 2022). The effectiveness of this mechanism is highly sensitive to the environment, as the addition of salts can shield these charges and reduce the Debye screening length (κ^{-1}), leading to a loss of protein stability and emulsion stability (McLauchlan et al., 2024).

2.3.3.2 Steric Stabilization

Steric stabilization arises from the physical presence of hydrated protein chains that project into the continuous phase, creating a mechanical barrier that prevents droplets from getting close enough to coalesce. This mechanism is robust than electrostatic repulsion as it is relatively insensitive to the presence of electrolytes. The most effective steric stabilizers are amphipathic molecules that consists of an “anchor” group which is nominally insoluble and stays attached to the oil droplet, and a “stabilizing moiety”, which must be soluble in the surrounding medium to remain extended (Napper, 1977).

2.3.3.3 Electrosteric Stabilization

An electrosteric stabilization is a strategy that combines electrostatic and steric stabilization (Capek, 2002). Chemical and enzymatic techniques, such as succinylation or deamidation, can effectively increase the net negative charge while simultaneously unfolding the protein structure (Ibrahim et al., 2022).

2.3.4 Foam Physics

Aqueous foams are dispersions of gas in liquid that evolve and decay through three mechanisms: liquid drainage, Ostwald ripening (coarsening), and coalescence (Denkov et al., 2020; Saint-Jalmes & Langevin, 2002).

2.3.4.1 Liquid Drainage

Liquid drainage occurs when the gravity pulls down the continuous phase through a network of interconnected channels, known as plateau borders and nodes leading to the thinning of the liquid films separating the bubbles (Saint-Jalmes & Langevin, 2002). This process is governed by the balance between gravitational forces and capillary action, and it is slowed down by high bulk viscosity or the formation of a viscoelastic surface layer (Denkov et al., 2020).

2.3.4.2 Ostwald Ripening

Ostwald ripening is the transfer of gas from smaller bubbles to larger bubbles due to internal pressure differences governed by the Laplace pressure (Langevin, 2025). Smaller bubbles have a higher chemical potential due to higher internal pressure, causing gas to diffuse through the thin liquid films (TLFs) toward larger bubbles with lower pressure. This results in a continuous increase in average radius of the bubbles over time (Saint-Jalmes & Langevin, 2002; Yazghur et al., 2018).

2.3.4.3 Coalescence

Coalescence is defined as the rupture of the thin liquid films separating the bubbles, which causes them to fuse into a single larger bubble (Yazghur et al., 2018). This is a thermally activated process that involves nucleation of holes in the adsorbed layers. The probability of coalescence is higher when the surface layer is less compact and the surface tension is high (Langevin, 2025). Stability against coalescence is maintained by the disjoining pressure, which is the sum of attractive van der Waals and the repulsive electrostatic forces that prevent the two bubble interfaces from coming in contact (Janssen et al., 2025; Langevin, 2025).

2.4 The Barista Challenge: Coffee-Oat Drink Interactions

2.4.1 Acidic and Thermal Stress

Utilization of oat proteins in mildly acidic food applications is limited due to their poor solubility under neutral and slightly acidic pH conditions (Li & Xiong, 2021). This instability is due to the structural heterogeneity of the oat 12S globulins, which shows a broad isoelectric point (*pI*) range between 4.5 and 7.5, with their constituent acidic subunits exhibiting *pI* between 4 and 5 (McLauchlan et al., 2024). This creates an isoelectric shock when oat drink is introduced to coffee (pH 4.7), which is an environment that falls within the *pI* range of the surface accessible α-subunits. At this specific pH, the net surface charge becomes zero, leading

to decreased repulsive forces and an increase in attractive forces that favour protein aggregation and visible curdling in the coffee (Vikenborg & Stensson, 2020). Even though the 12S globulin exhibits a high peak denaturation temperature (≈110°C), thermal stress in the range used for barista steaming (60-70°C), induces partial unfolding and subunit dissociation that exposes the buried hydrophobic patches on the 12S globulin. This results in aggregation especially under the acidic conditions of coffee (McLauchlan et al., 2024; Shen et al., 2025).

2.4.2 Polyphenol-Protein Interactions

Interactions between proteins and chlorogenic acid (CGA) are categorized into two main groups: covalent (chemical or irreversible) and non-covalent (physical or reversible) linkages. These interactions can significantly modify the protein structure and functionality (Tarahi et al., 2024). CGA have high affinity for binding with proteins, specifically reacting with nucleophilic amino acid residues such as the ϵ-amino group in lysine, the thiol group in cysteine, and tyrosine residues (Pan et al., 2022). Coffee polyphenols exhibit a thermodynamically favourable affinity for proline residues, where the π-conjugated moiety of the polyphenol interacts with the aliphatic moiety of the proline side chains through hydrophobic interactions (Horita et al., 2025). Studies show that, binding of CGA to proteins results in a decrease in ordered α-helix and β-sheet structures and an increase in disordered random coils leading to a structural transition (Pan et al., 2022).

3. Materials and Methods

3.1 Materials

3.1.1 Ingredients and Enzymes

De-hulled and heat-treated Swedish oat kernels (*Avena sativa*), specifically a standard trade blend of mixed varieties, provided by Cerealiq AB (Bjuv, Sweden) served as the raw material for all the laboratory prepared oat drink samples. The enzyme treatment was performed using specific enzyme systems also supplied by Cerealiq AB, comprising two types of amylases (Amylase 1 and Amylase 2) and four types of proteases (Protease 1, 2, 3, and 4).

For the formulation of oat drink samples, food-grade rapeseed oil (ICA, Svensk Rapsolja)) was used as the lipid source. The minerals and salts used for stabilizing and fortifying the oat drink included sodium chloride (regular kitchen salt), calcium carbonate ($CaCO_3$), and dipotassium phosphate (K_2HPO_4). Analytical grade chemicals were used for all protein tests, including the bicinchoninic acid (BCA) assay and sodium dodecyl sulfate-polyacrylamide gel electrophoresis (SDS-PAGE).

3.1.2 Commercial Reference Samples

To establish a performance benchmark, four commercially available oat drinks were included in the study. These samples were selected in consultation with Cerealiq AB based on their market prevalence in Sweden and their positioning in the market as either “barista-grade” or “standard” oat drinks. The beverages were purchased from local retailers in Lund, Sweden, and stored under refrigerated conditions (4°C) prior to analysis. The reference sample included were:

i. Oatly Oat Drink Barista Edition
ii. Oatly Oat Drink Organic
iii. Fazer Aito Oat Drink Barista
iv. ICA Oat Drink Barista

3.2 Preparation of Oat Drink Sample

The preparation of all oat drink samples was conducted at the facilities of Cerealiq AB according to a standardized protocol to ensure consistency across all experimental trials. To

ensure the reproducibility of the enzymatic modification and formulation processes, each of the six enzyme treatments was performed in three independent batches (n=3).

3.2.1 Milling and Slurry Preparation

Whole oat groats were ground into a fine powder using a grinder (Melitta Calibra). To prepare the initial slurry, 1600 g of water was dispersed into 200 g of the resulting oat flour. The water phase is a mix of 1100 g of boiling water and 500 g of water at room temperature, achieving a starting temperature of 68-70°C. The mixture was blended thoroughly using a hand blender to ensure uniform hydration of the flour before enzymatic treatment.

3.2.2 Enzymatic Hydrolysis and Viscosity Monitoring

The enzymatic treatment was initiated by introducing the specific combinations of amylases and proteases (Table 3.1.) into the mixture. The enzymes were added in varying proportions according to the technical guidance and formulation strategies of Cerealiq AB. Due to the proprietary reasons, the exact enzyme dosages are not disclosed.

Table 3.1: Experimental design and enzyme combinations for oat drink samples.

Sample Name	Protease Component	Amylase Component
Sample 1 (S1)	Protease 1	Amylase 1
Sample 2 (S2)	Protease 2	Amylase 1
Sample 3 (S3)	-	Amylase 1
Sample 4 (S5)	Protease 3	Amylase 1
Sample 5 (S6)	Protease 4	Amylase 1
Sample 6 (S7)	Protease 4	Amylase 2

The hydrolysis was performed for a period of 60-minute under constant mechanical agitation. Stirring was maintained at a fixed speed of 120 RPM using an overhead stirrer (Hei-TORQUE 100, Heidolph, Germany). To ensure precise temperature control, the reaction vessel was submerged in a regulated water bath maintained at 68°C throughout the process. During the

hydrolysis, the apparent viscosity of the slurry was monitored at 15-minute intervals to track the progress of the reaction. At each interval, a portion of the sample was withdrawn and cooled to a standardized temperature of 25°C prior to analysis. Viscosity measurements were conducted using a rotational viscometer (DVPLUS LV, AMETEK Brookfield, USA) equipped with an LV-02 (62) spindle operating at a constant speed of 60 RPM. Following the 60-minute hydrolysis, the mixture was immediately boiled for 2 minutes to ensure the complete inactivation of the enzymes and to terminate the reaction.

3.2.3 Filtration and Formulation

The inactivated hydrolysed oat drink was passed through a two-step sieving process using 500 µm and 200 µm mesh sieves to separate the insoluble fibre from the liquid fraction. After filtration, each enzyme-treated batch was divided into two distinct portions for a comparative study of the protein's behaviour before and after ingredient addition.

One portion was maintained in its raw, unformulated state and designated as the "Base" (B) sample (e.g., S1B). The other portion, which was modified to achieve desired barista-grade sensory and functional properties, was designated as the "Formulated" (F) sample (e.g., S1F). The formulation process involved the addition of rapeseed oil, sodium chloride, calcium carbonate, and dipotassium phosphate.

3.2.4 Final Processing and Storage

The formulated samples were subjected to heat treatment by boiling for 2 minutes to ensure complete integration of the added ingredients. To stabilize the resulting oil-in-water emulsion and achieve a uniform particle size distribution, the formulated samples were subjected to high shear homogenization using a high-shear mixer (T18 digital ULTRA-TURRAX, IKA-Werke GmbH &Co.KG, Germany) at a constant speed of 12,000 RPM for a duration of 5 minutes. Both the base and formulated samples were transferred to bottles and stored under refrigerated conditions at 4°C and were analysed within 4-5 days of production, during which they were considered fresh.

3.3 Physicochemical and Protein Characterization

3.3.1 Moisture Content and Total Solids

The moisture content of the Base (B) samples was determined to determine the total solids concentration resulting from the enzymatic treatments. Analysis was performed using a

moisture analyser (Kern DBS 60-3, KERN & SOHN GmbH, Germany). Approximately 2.0 g of each sample was heated at 120°C until a constant weight was achieved. The analysis was performed in triplicate using the dry matter method (%DC).

3.3.2 pH Measurement

The pH of both the Base (B) and Formulated (F) samples was measured at room temperature using a pH meter (FiveGo™ FG2, Mettler-Toledo International Inc., Greifensee, Switzerland). The electrode was calibrated using a two-point calibration with standard buffer solutions at pH 4.0 and 7.0 prior to measurement.

3.3.3 Soluble Protein Content (BCA Assay)

The concentration of soluble protein in the Base (B), Formulated (F) and Commercial (C) samples was quantified using the bicinchoninic acid (BCA) assay with a commercial Pierce™ BCA Protein Assay Kit (Thermo Fisher Scientific, Rockford, IL, USA). To isolate the soluble fraction, samples were subjected to centrifugation at 10,000×g (RCF) for 15 minutes at 4°C (Heraeus Megafuge 16R, Thermo Scientific, Germany) and the supernatant was carefully collected to exclude the insoluble fibre and the cream layer. The supernatants were diluted 1:10 in ultrapure water (Synergy® UV Water Purification System, Merck Millipore, France) to ensure the absorbance values remained within the linear working range of the assay. Standards were prepared using Bovine Serum Albumin (BSA) in a concentration range of 0 to 2000 µg/mL.

The assay was performed using a 96-well microplate guide. A 25 µL aliquot of each standard and dilutes sample was mixed with 200 µL of the working reagent. The plate was shaken for 30 seconds and then incubated at 37°C for 30 minutes (SPECTROstar Nano microplate reader, BMG LABTECH, Ortenberg, Germany). Following incubation, absorbance was measured at 562 nm. All measurements were blank-corrected and each independent batch was analysed in triplicate. The final protein concentrations were calculated using the standard curve and corrected for the 1:10 dilution factor.

3.3.4 Surface Charge (Zeta Potential)

The surface charge of the colloidal particles in the beverages was determined by measuring the zeta-potential using Zetasizer Nano ZS (ZEN3600, Malvern Panalytical, Malvern, UK). Measurements were performed on supernatants obtained by the centrifugation process (10,000×g for 15 minutes at 4°C) described in Section 3.3.3. To ensure optimal attenuation and

avoid multiple scattering effects, the supernatants were diluted in ultrapure water based on their relative turbidity. The Base (B) samples and Oatly Oat Drink Organic were diluted 1:100, while the Formulated (F) samples and the remaining commercial benchmarks were diluted 1:1000.

The refractive index (RI) for the particles was set at 1.450 due to the composite nature of the protein-stabilized emulsion (Kayeye et al., 2025). The RI of the dispersant (water) was set at 1.330 with a viscosity of 0.8872 cP. Measurements were conducted at 25°C using a folded capillary cell (DTS1070) after a 120-second equilibration period. The instrument calculated zeta-potential from the measures electrophoretic mobility using the Smoluchowski model. Each independent samples were analysed in triplicate.

3.3.5 Particle Size Distribution

The particle size distribution (PSD) of the oat drinks was determined via laser diffraction using a Mastersizer 2000 (Malvern Panalytical, Malvern, UK) equipped with a Hydro 2000SM wet dispersion unit. The optical properties were set using a RI of 1.470 for the particles and an RI of 1.330 for the dispersant and the system operates with a dual-laser configuration (He-Ne laser at 633 nm and blue solid-state diode laser at 466 nm). The samples were introduced dropwise into the Hydro dispersion unit containing ultrapure water until a target obscuration level of 14-15% was achieved. A constant stirring speed of 1450 RPM was maintained throughout the analysis to ensure homogeneity. The PSD was calculated based on the Mie scattering theory, assuming spherical particles and results were obtained as the volume-weighted mean diameter.

3.3.6 Sodium Dodecyl Sulfate-Polyacrylamide Gel Electrophoresis (SDS-PAGE)

The molecular weight distribution and extent of proteolysis were analysed via Sodium Dodecyl Sulfate-Polyacrylamide Gel Electrophoresis (SDS-PAGE) under reducing conditions. The Base (B) samples were first clarified (10,000 × g, 5 min, 4°C) and were normalized to a constant protein load (based on BCA results). The normalized supernatants were then mixed 1:1 with 4x Laemmli sample buffer containing 5% (v/v) β-mercaptoethanol (Bio-Rad Laboratories, USA) and denatured at 100°C for 5 minutes. Sample were cooled and 15 µL of each sample was loaded into the wells of a Mini-PROTEAN TGX Stain-Free precast gel (4-15% gradient) (Bio-Rad Laboratories, USA). Electrophoresis was run in a Mini-PROTEAN Tetra system (Bio-Rad Laboratories, USA) with 1x TGS buffer at a constant 200 V for approximately 45 minutes. Precision Plus Protein Dual Colour Standards was used as the molecular weight marker. After the run, protein bands were visualized using a ChemiDoc MP+ imaging system.

3.3.7 Interfacial Properties: Dynamic surface tension and modulus of elasticity

The air-liquid surface tension (γ) of the oat drinks was determined using the pendant drop technique. Measurements were performed on the supernatants (10,000 × g, 15 min, 4°C) using a Tracker^{TM} tensiometer from Teclis (Lyon, France) equipped with WINDROP software. A Teflon-treated syringe was used and the drop volume was set to 8 µL. The analysis was conducted at a constant temperature of 25°C. The surface tension was monitored for a duration of 600 seconds to reach an equilibrium state. The software calculates the surface tension in real-time by fitting the drop profile to the Young-Laplace equation:

$$\Delta P = \sigma\left(\frac{1}{R_1} + \frac{1}{R_2}\right) \quad (1)$$

where σ is the surface tension, R_1 and R_2 are the principal radii of curvature, and ΔP is the pressure difference across the interface. Each of the three independent batches (n=3) was analysed in triplicate.

3.3.8 Microstructural Analysis

Light microscopy was performed on the Formulated (F) samples to characterize the microscopic difference between the three distinct phases: the top (cream) layer, the middle (serum) layer, and the bottom (sediment) layer, formed after keeping the samples undisturbed overnight in refrigerated condition. For each sample, a small aliquot was carefully withdrawn from each layer and placed on a glass microscope slide with a coverslip. Observations were conducted using an Olympus BX50 light microscope (Olympus Corporation, Japan) at a magnification of 10**x.**

3.4 Functional Barista Performance

3.4.1 Emulsion and Sedimentation Stability

The physical stability of the formulated (F) samples was evaluated through a static separation test. A 100 mL aliquot of each sample was transferred into a graduated cylinder and stored in refrigerator (4°C) overnight. The degree of stability was quantified by recording the volumes (mL) of the resulting phases: the top cream layer, middle serum layer, and the bottom sediment layer.

3.4.2 Foaming Capacity and Stability

The foaming performance was assessed using a standardized mechanical aeration method. A 100 mL aliquot of the formulated oat drink was frothed using a Nespresso Aeroccino 4 (Nestlé Nespresso S.A., Lausanne, Switzerland). The resulting foam and liquid volumes were measured in a graduated cylinder after 30 seconds and 10 minutes. These measurements were used to calculate the following parameters:

Foaming Ability (%): This represents the proportion of foam within the total volume:

$$\text{Foaming Ability (\%)} = \left(\frac{Total\ Volume - Liquid\ Phase\ Volume}{Total\ Volume}\right) \times 100 \quad (2)$$

Volume Increase: This measures the expansion of the sample relative to the initial 100 mL volume:

$$\text{Volume Increase} = \frac{Total\ Volume\ at\ 30\ seconds}{Initial\ Liquid\ Volume\ \ (100\ mL)} \quad (3)$$

Foam Stability Index (FSI): The stability of the foam was quantified by the retention of the total volume over a 10-minute period:

$$\text{FSI} = \left(\frac{Total\ Volume\ at\ 10\ minutes}{Total\ Volume\ at\ 30\ seconds}\right) \times 100 \quad (4)$$

3.4.3 Coffee Stability

To simulate real-world barista application, the compatibility of the oat drinks with hot, acidic coffee was evaluated. Coffee was prepared using a drip machine with a standardized ratio of 35 g of ground coffee (ICA Basic) to 518 g of water, resulting in a brew with a pH of 4.71. A 25 mL portion of the oat drink was added to 50 mL of coffee maintained at 64-65°C. The mixture was visually inspected for signs of feathering, flocculation, or emulsion breakdown at intervals of 5 and 10 minutes after mixing. The results were documented photographically using a smartphone (Samsung S20 FE).

3.5 Statistical Analysis

Statistical analyses were performed using the "Data Analysis" Toolpak in Microsoft Excel 2021 (Version 2604, Microsoft Corp., Redmond, WA, USA). One-way and two-way analysis of variance (ANOVA) were employed to evaluate the differences among experimental groups.

Prior to performing ANOVA, the data were validated for homogeneity of variances through descriptive statistics. Results were considered statistically significant when $p < 0.05$.

4. Results and Discussion

4.1 Enzymatic Hydrolysis Kinetics and Viscosity Reduction

The enzymatic treatment of the oat slurry was conducted to achieve liquefaction which is crucial for producing a stable PB beverage. The hydrolysis process breaks down complex oat matrix resulting in decrease of viscosity. Treatment time also influences the liquefaction process (Deswal et al., 2014). From an industrial perspective, a lower viscosity is preferred to facilitate ease of processing, while a higher viscosity is essential for the creamy mouthfeel expected in barista-grade products without the use of thickeners (Bhokarikar et al., 2024).

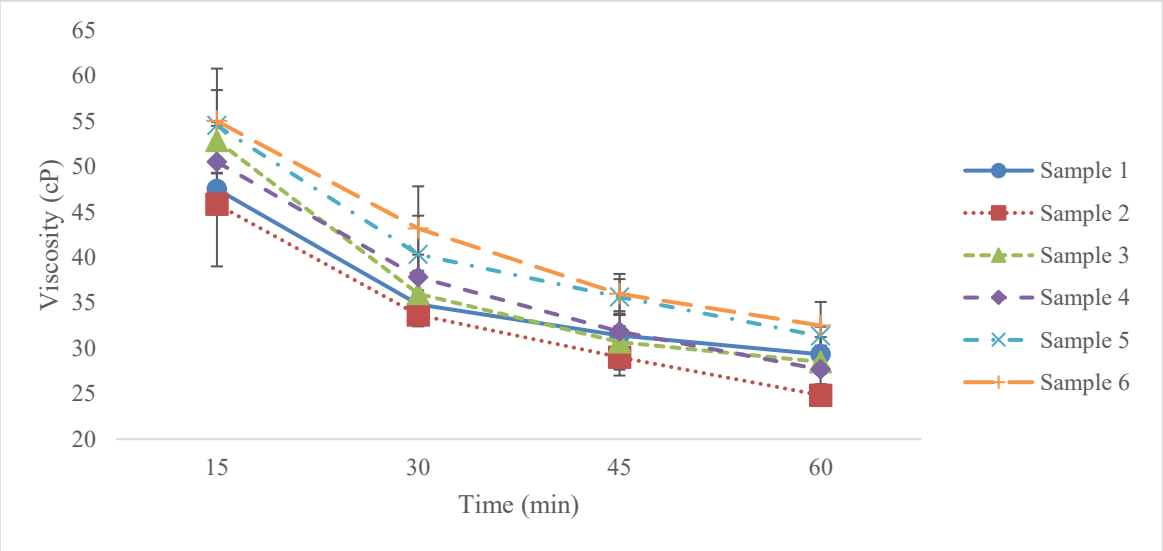

Figure 4.1.: Viscosity reduction kinetics of oat slurry during-60-minute enzymatic hydrolysis (n = 3)

As illustrated in *Figure 4.1.,* all six experimental treatments demonstrated a consistent reduction in viscosity throughout the 60-minute hydrolysis. The narrowing of error bars observed in *Figure 4.1.* as time progressed to 60 minutes indicates that the slurry reached a highly predictable and reproducible terminal state for all enzyme combinations. The most rapid reduction occurred within the first 15-30 minutes (Phase 1), followed by a plateauing effect from 30-60 minutes (Phase 2). This trend aligns with the findings of Deswal et.al (2014), which states that the conversion of starch to dextrin results in a significant decrease in viscosity.

The terminal viscosity values at 60 minutes varied significantly across the treatments (p = 0.0016), as shown in *Figure 4.2.* Sample 2 and Sample 3 exhibited the highest viscosity reduction efficiency, both reducing relative viscosity by approximately 46% over the 60-minute

period. Sample 2 achieved the lowest absolute terminal viscosity (24.8 ± 1.04 cP), marking it as the most aggressive liquefaction treatment. In contrast, Sample 6 and Sample 5 resulted in the highest terminal viscosities (32.5 ± 2.6 and 31.3 ± 1.04, respectively). Sample 4 achieved an intermediate terminal viscosity of 27.7 cP. Sample 1 demonstrated a unique kinetic profile. While it showed the lowest relative hydrolysis rate (61.7%), it reached a terminal viscosity of 29.3 ± 1.89. The unique viscosity profile of Sample 1 and the high terminal viscosity of Samples 5 and 6 suggest different levels of structural modifications as Deswal et al. (2014) suggest viscosity is not just determined by starch but is influenced by the entire colloidal matrix.

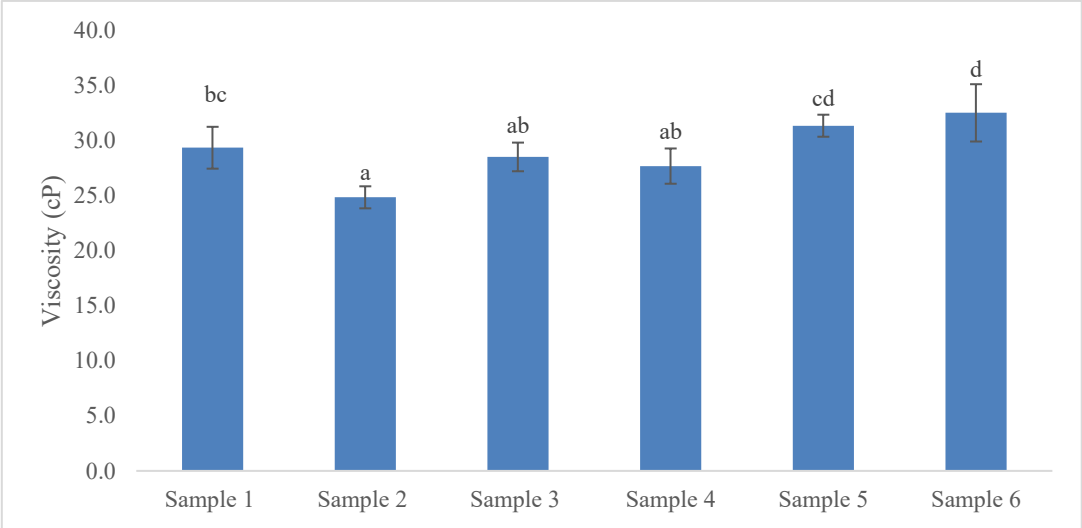

Figure 4.2: Terminal viscosity of oat drinks after 60 minutes of hydrolysis. Error bars represent the standard deviation (n=3). Superscript letters (a-d) indicate statistical groupings based on Tukey's HSD post-hoc test ($p<0.05$). Samples that share at least one common letter are not statistically different from each other. Conversely, samples that do not share any common letter are significantly different

4.2 Protein Structural Modification

To investigate how enzymatic treatments modified the oat protein at a molecular level, a combination of SDS-PAGE and BCA assay was employed.

4.2.1 Molecular Weight Distribution (SDS-PAGE)

The molecular weight distribution and the extent of proteolysis were analysed using SDS-PAGE reducing conditions, as shown in *Figure 4.4*. The electrophoretic profile helps to characterize the structural transition from native proteins to hydrolysed peptides. Following the characterisation established by X. Wang et al. (2022), the native oat protein profile (represented here by Sample 3, which contain only amylase) is dominated by the 12S globulin, also known as avenalin. As identified in Section 2.1.1 of the theoretical background earlier, these storage proteins appear as two distinct groups of subunits, the acidic polypeptides (12S-A) with a

molecular weight of ~32-35 kDa and the basic polypeptides (12S-B) at ~22kDa. These bands are clearly visible and sharp in Samples 3, 4, 5, and 6, indicating that the primary structure of the subunits remained intact under these specific enzyme treatments. The presence of faint bands near 65 kDa and below 15 kDa corresponds to 7S and 3S protein fractions respectively, which are minor storage proteins in oats as confirmed by X. Wang et.al (2022) and Shay et.al (2023).

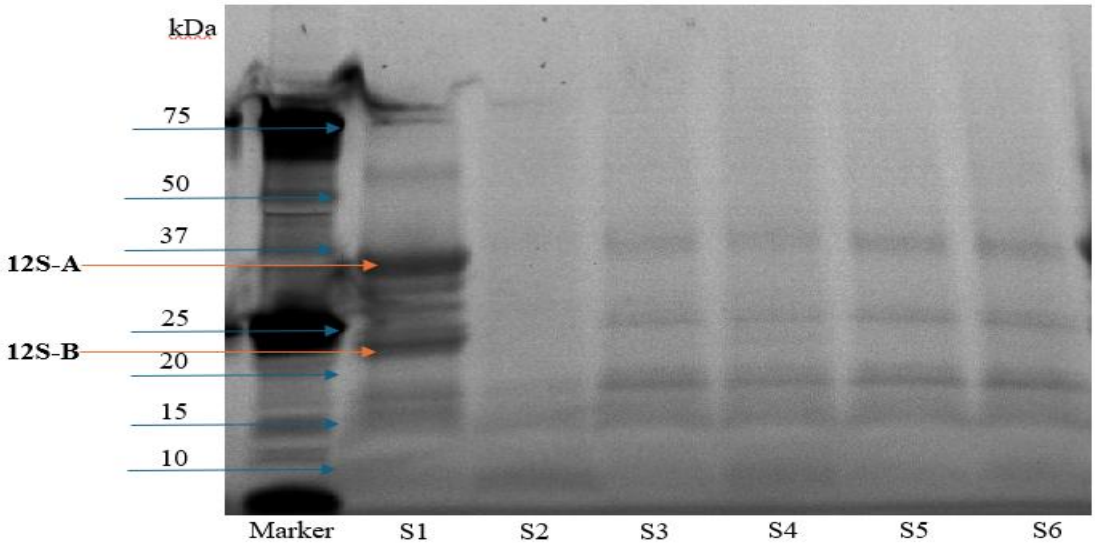

Figure 4.4.: SDS-PAGE (4-15% gradient) of oat protein hydrolysates under reducing conditions. Lane 1: Molecular weight marker (kDa); Lane 2: Sample 1; Lane 3: Sample 2; Lane 4: Sample 3; Lane 5: Sample 4; Lane 6: Sample 5 and Lane 6: Sample 6. All lanes were normalized to a protein load

The six experimental treatments revealed significant difference in proteolytic efficiency. As shown in Figure 4.4, Sample 1 exhibited the highest visual intensity and a pronounced vertical smear. Although the loading was normalised to the same protein load based on the BCA results, this high intensity reflects the high protein yield of the Protease 1 treatment, which likely resulted in a high local protein density in the well. This suggests that Protease 1 effectively released the protein from the complex oat matrix. Nieto-Nieto et al. (2024) suggest that partial hydrolysis can shift bands to lower molecular weight regions (26-34 kDa), altering the balance between electrostatic repulsive forces and hydrophobic attractive forces. According to Li and Xiong (2023), such structural modifications occurring without the total loss of primary subunits enhances molecular flexibility, allowing the released polypeptides to spontaneously organise at the interface to form a viscoelastic film.

Conversely, Sample 2 showed a high degree of proteolytic aggression, resulting in a disappearance of nearly all major protein bands. This indicates that Protease 2 achieved extensive hydrolysis, cleaving the 12S globulins into peptides smaller than the detection limit (likely <10 kDa). While this indicates high enzymatic activity, Nieto-Nieto et.al (2014), also observed that excessive hydrolysis can lead to weak colloidal structure due to drastic reduction in the size of the protein molecules. Finally, the protein profiles of Samples 4,5, and 6 remained almost similar to Sample 3, which contains only Amylase. This suggests that Protease 3 and Protease 4 did not significantly alters the molecular weight of the 12S globulin subunits.

4.2.2 Soluble Protein Concentration (BCA Assay)

The BCA assay was used to quantify the concentration of protein extracted from the insoluble oat matrix into the liquid phase. As shown in *Figure 4.3.*, two-factor ANOVA confirmed that both the choice of enzyme (variation between samples) and the formulation process (variation within each sample from base to formulated state) exerted a significant impact on the final concentration of the soluble protein ($p < 0.05$). Specifically, the formulation process showed a highly significant increase in protein solubility across all treatments ($p < 0.001$).

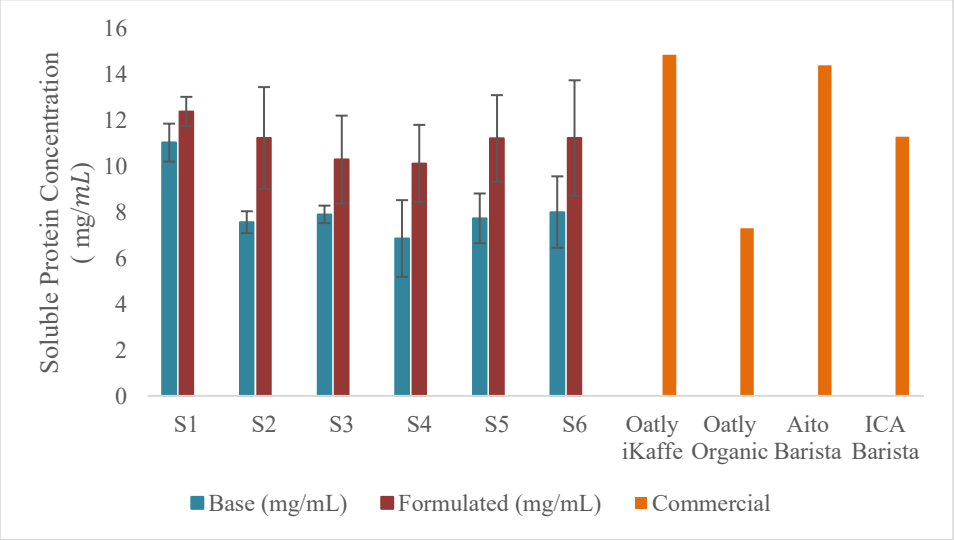

Figure 4.3.: Effect of enzyme treatment and formulation on soluble protein concentration (mg/mL)

Statistical analysis of the experimental data confirmed that the choice of enzyme is a critical factor in determining the protein yield of the drink, with a significant effect observed across the treatments ($p = 0.0322$) (See App. 4). Sample 1 showed the highest protein solubility (11.04 mg/mL) among all experimental base samples. This aligns with the findings of Ibrahim et al. (2022), which state that limited proteolytic hydrolysis is highly suitable for unfolding the

complex structure of native oat protein to promote its solubility. As discussed by Shay et.al (2023), effective hydrolysis also increases solubility by producing small-sized polypeptides (<15 kDa for oat) and exposing hydrophilic areas, including ionic and polar amino groups. Thus, Protease 1 likely altered the native globulin conformation and increased protein solubility by changing secondary and higher order structure (as confirmed by the SDS-PAGE results), consistent with reports that enzymatic hydrolysis improves the functional solubility of plant proteins (J. Wang et al., 2022; Wouters et al., 2016).

In contrast, Sample 2 presented a notable reduction in soluble protein content (7.57 mg/mL) despite being the most aggressive enzymatic treatment (as confirmed from SDS-PAGE results). This is supported by Zhang et al. (2017), who reported that during extensive proteolysis, the aggregation of peptides can take place, resulting in significant reduction of protein extractability. Shay et.al (2023) further suggest that high protein concentrations can strengthen these protein-protein interactions.

The remaining samples further show the impact of enzyme specificity on protein extraction yield. The results for Sample 3, which utilized only amylase, show that starch liquefaction alone is insufficient to maximize protein solubility as the native globular confirmation remains intact and resistant to water interaction (Shay et al., 2023). The comparatively lower solubility of Sample 4 suggests that the Protease 3 system was less effective in cleaving the acidic peptide chains required to expose the hydrophilic areas (Shay et al., 2023; Wouters et al., 2016). The comparatively higher soluble protein content in Sample 5 and Sample 6 demonstrates the efficacy of Protease 4 in modifying the structure.

The formulated samples showed a highly significant increase in soluble protein across all treatments ($p < 0.001$). This can be attributed to the addition of dipotassium phosphate and sodium chloride resulting in an increase in pH (from ~6.7 in the base to ~7.7 in formulated samples). Hu et al. (2025) noted that the stabilization of oat drink is significantly improved under neutral and alkaline condition. When benchmarked against commercial standards, formulated Samples 1 and 6 were highly competitive matching the soluble protein levels of Aito Barsita.

4.3 Physicochemical Properties: pH and Zeta Potential

4.3.1 pH

The pH of an oat beverage strongly influences its colloidal behaviour. As illustrated in *Figure 4.2.*, a distinct shift in pH was observed across all treatments, where the formulation process increased the pH of every sample by approximately 1.0 unit. The samples ranged from pH 6.64 ± 0.06 to 6.94 ± 0.14, while the formulated samples shifted to a distinctly alkaline range of 7.91 ± 0.10 to 7.81 ± 0.08. Statistical analysis via Two-Factor ANOVA confirmed that this shift was highly significant ($p = 2.97 \times 10^{-19}$), while differences between the specific enzyme treatments were also significant ($p = 0.023$).

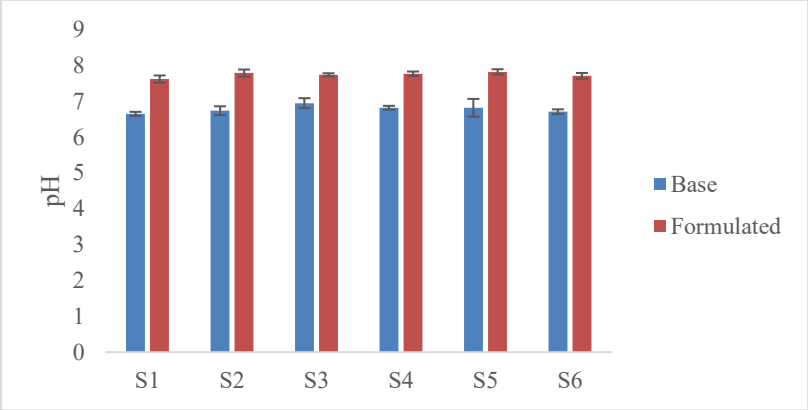

Figure 4.5.: pH values of Base and Formulated oat drink samples (n=3)

According to McLauchlan et al. (2024), oat proteins exhibit a characteristic U-shaped solubility profile, with minimum solubility occurring near the *pI* of 4.5 to 5.0. By utilizing dipotassium phosphate and calcium carbonate as buffering agents, the formulation successfully shifted the system to the alkaline condition. This alkaline environment promotes the deprotonation of carboxylic acid groups on the amino acid side chains and increase the net negative charge. This can help in preventing feathering or curdling normally observed when PB drinks are introduced to acidic coffee (pH ≈ 4.7). Notably, Sample 3 exhibited the highest base pH (~ 6.94), whereas samples treated with proteases showed lower values, likely due to the release of acidic amino acid chains or the exposure of carboxylic groups during proteolysis.

To further evaluate the relationship between the sample's electrostatic environment and the efficiency of protein solubility, a correlation analysis was performed between pH and soluble protein concentration (*Figure 4.6.*). The results showed a clear separation between "Base" and "Formulated" samples validating the solubility trends described by McLauchlan et al. (2024). By moving the system from pH ~6.7 to ~7.7, the formulation effectively shifts the oat proteins

further up the right-hand side of the solubility curve. However, the intra-group correlation coefficients ($R^2 \approx 0.35$) within both groups indicate pH alone does not result in the variation in solubility suggesting the secondary influence of enzyme specificity.

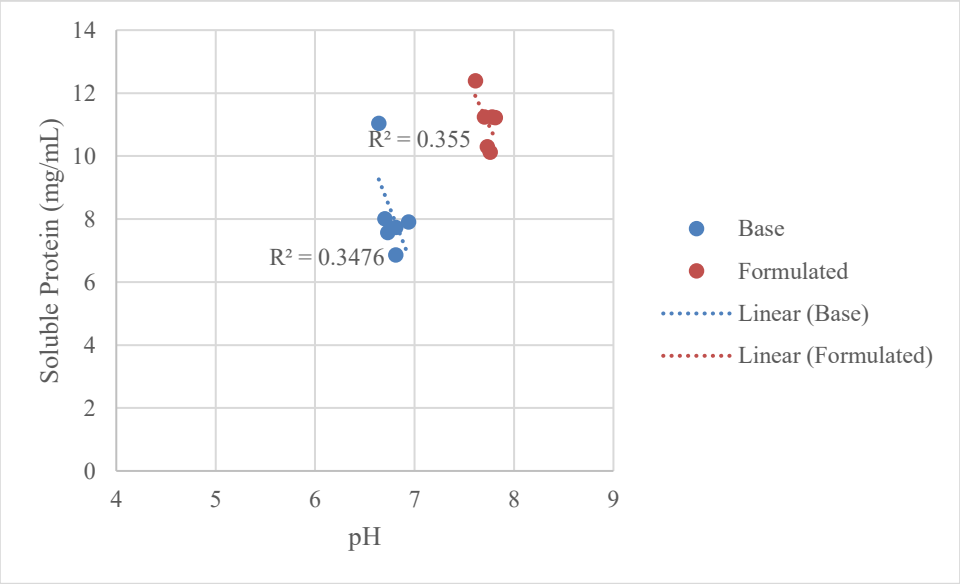

Figure 4.6.: Correlation between sample pH and soluble protein concentration (mg/mL)

4.3.2 Surface Charge and Zeta Potential

To assess the likelihood of colloidal aggregation and characterise the electrostatic repulsion surrounding oat particles, the zeta potential (ZP) was measured for all samples. As shown in *Figure 4.7.*, all formulated experimental samples (S1F-S6F) exceeded the -30mV threshold generally required for strong electrostatic stabilization in biological emulsions (Sharma et al., 2014). Statistical analysis revealed that the type of enzyme had a significant impact on the resulting surface charge ($p = 0.00025$), and the formulation process further enhanced the negative charge magnitude ($p = 0.012$).

Among the base samples, Tukey's HSD test revealed significant statistical differences between the enzyme treatments. Sample 6B (-39.40 mV, Tukey letter 'a' was identified as the most stable base, statistically superior to the least stable base, Sample 2B (-27.83 m, Tukey letter 'b'). According to Immonen et al. (2022), enzymatic modification increases the negative surface charge by converting glutamine and asparagine residues into glutamic and aspartic acid. Protease 3 and 4 (Samples 4B, 5B, and 6B) appeared more effective at unfolding the native protein to expose the surface-active groups compared to the aggressive cleavage observed in Sample 2B. This aligns with earlier discussion in Section 4.2.1, suggesting excessive hydrolysis

can lead to reduction in charge density if the resulting peptides are too small to maintain a robust surface-active layer.

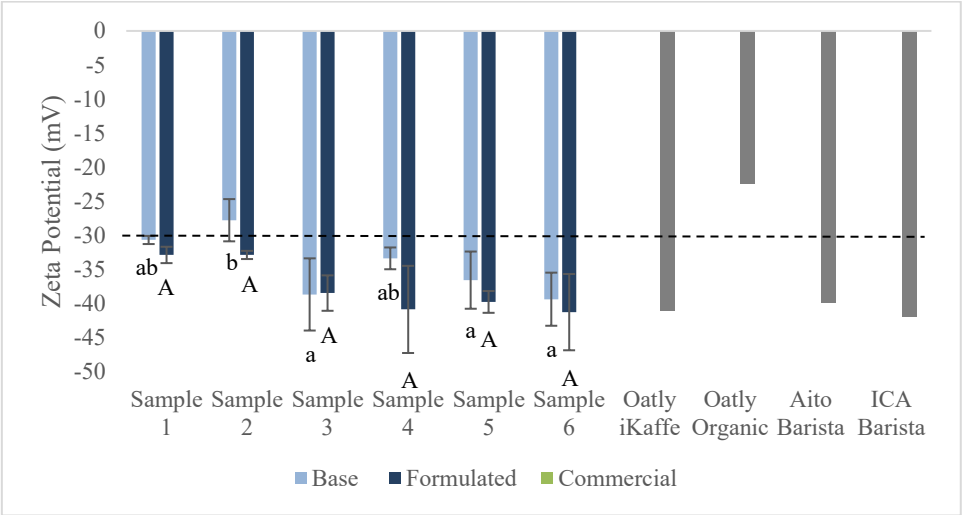

Figure 4.7: Zeta potential (mV) of experimental samples and commercial benchmarks. Experimental samples are categorized into Base (Tukey letters a, ab, b) and Formulated (Tukey letter A) groups. The dashed line at -30 mV indicates the threshold for strong electrostatic stabilization.

Statistical analysis of formulated samples (S1F-S6F) showed they are statistically similar (p >0.05). Although Sample 6F showed a higher negative ZP (-41.27 mV) compared to Sample 1F (-32.90 mV), the difference did not reach significance. This suggests that addition of salts elevated the colloidal stability of all experimental samples regardless of the initial enzyme treatment. Despite achieving highest protein solubility, Sample 1 showed lower ZP magnitude compared to Sample 6. This suggests that while Protease 1 was most efficient at releasing protein from the oat matrix into the liquid phase, the proteases in Samples 4 and 6 were more effective at increasing surface charge density of individual particles. It is likely that the larger, polydisperse peptide fragments provides a synergistic combination of moderate electrostatic repulsion and steric stabilization in Sample 1.

When benchmarked against commercial standards, Sample 4F and Sample 6F effectively matched the Oatly iKaffe (-41 mV). However, the Oatly organic sample showed the lowest negative ZP in the study (-22.4 mV). This can be attributed to its higher conductivity (0.044 mS/cm) compared to the more stable barista-friendly samples. As described by McLauchan et al. (2024), high conductivity results in ion shielding, where excess ions crowd around the protein particles and mask their charge. This reduces the Debye screening length, weakening the electrostatic repulsion and making the system prone to aggregation. Ultimately, the results confirm that a combination of optimized proteolysis and alkaline buffering is essential to achieve the industrial level stability in oat drink.

4.4 Particle Size Distribution

Particle size distribution (PSD) is an indicator of the physical stability of PB beverages. As established by Zhou et.al (2023), sedimentation of oat drink is heavily influenced by the particle size, where a smaller diameter and a narrow distribution are generally preferred to obtain stable suspensions. The experimental samples in the study exhibited a characteristic trimodal distribution, representing the finest emulsified oil droplets and small peptides (< 1 μm), the main population of protein-stabilized oil droplets (2-15 μm), and larger macro-aggregates or insoluble fibre particles (Figure 4.8.) (>30 μm) (Pei et al., 2021; Sridharan et al., 2020). The physical nature of this particle populations was visually validated through light microscopy of the top, middle, and bottom layers. Representative micrographs and further discussion on the colloidal heterogeneity across all treatments are provided in Appendix B.

One-way ANOVA conducted on the volume mean diameters ($d_{4,3}$) revealed a highly significant difference between the enzyme treatments (p = 0.00067). This confirms that specific enzyme treatment was the primary determinant of the final particle size. Sample 1 achieved the lowest mean diameter (24.53 ± 0.29 μm), primarily due to the absence of the large macro-aggregate peak (> 100μm) found in other samples. Here, it is essential to consider that the PSD represents a composite of various species, including protein-stabilized oil droplets, protein aggregates, and insoluble fibre residues, each with different densities and settling behaviour.

In contrast, Sample 2 showed a higher mean diameter of 51.08 ± 4.28 μm. This significant increase can be attributed to the higher volume distribution (2.87% of total volume) at the 100 μm peak. This can be correlated with the molecular structure of Sample 2 identified in the SDS-PAGE analysis. As established by Zhou et al. (2023), proteins function as emulsifiers that wrap oil droplets to provide steric stabilization and prevent aggregation. As discussed in Section 4.2.2, excessive hydrolysis likely reduced the oat globulins into smaller peptides with low molecular weight and structural integrity required to form a cohesive viscoelastic film around the oil droplets. This can result in rapid coalescence of oil droplets leading to the formation of the large 100 μm aggregates observed in the PSD graph.

The remaining samples (S3-S6) showed intermediate mean diameters ranging from approximately 39 to 40 μm. However, while the volume mean diameter was lowest for Sample 1 due to lesser large insoluble residues, visual assessment via light microscopy (Appendix B) suggests that Samples 5 and 6 possessed the most refined emulsion. Sample 6 exhibited a uniform dispersion of individual oil droplets that appeared smaller and more distinct than those

in Sample 1. This shows that enzymatic action of Protease 4 was more effective at stabilizing the oil-water interface, creating a population of fine droplets that are less prone to coalescence.

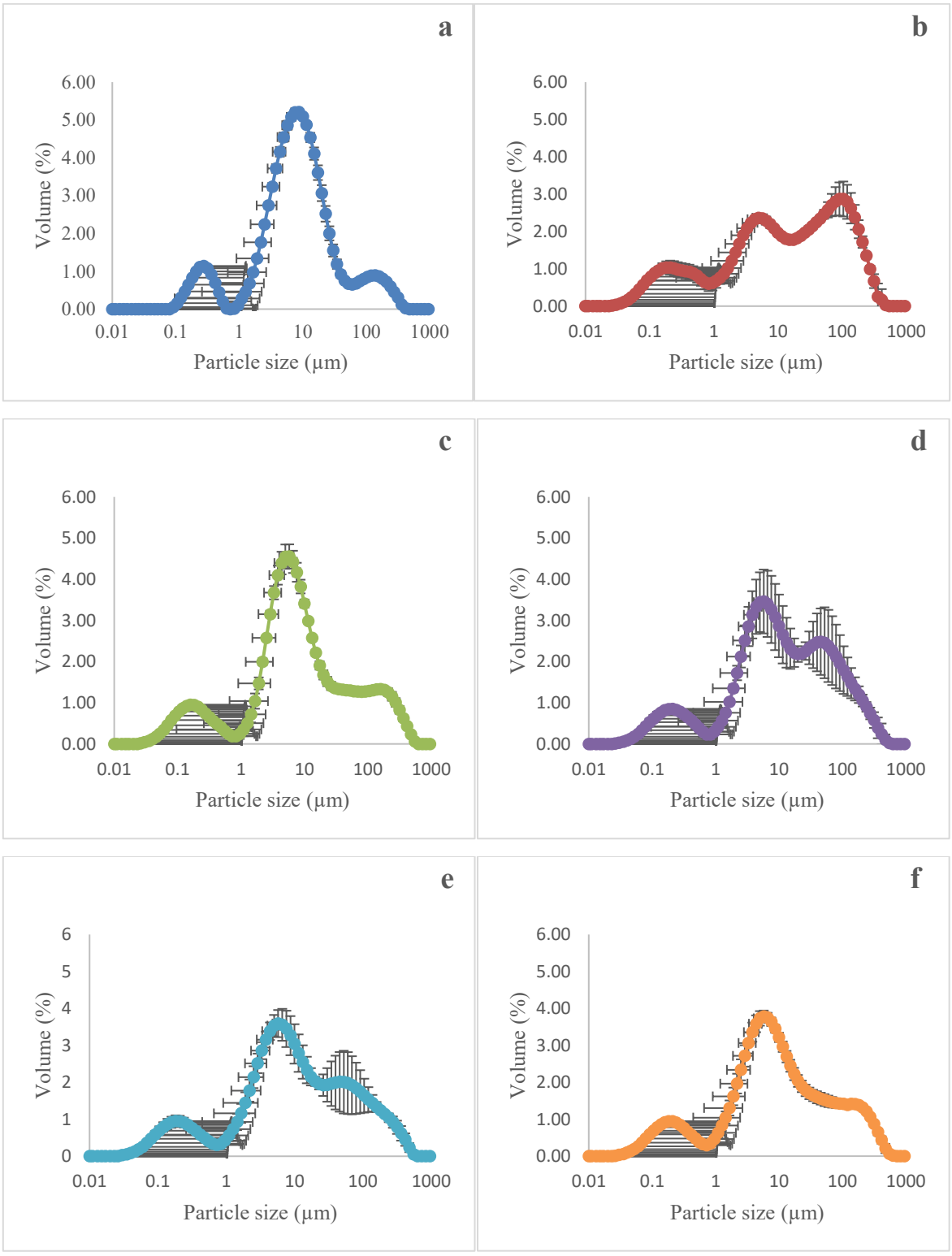

Figure 4.8.: Volume based particle size distribution (%) of formulated oat drink; (a) Sample 1F, (b) Sample 2F, (c) Sample 3F, (d) Sample 4F, (e) Sample 5F, and (f) Sample 6

4.5 Interfacial Behaviour and Foaming

The adsorption kinetics of oat proteins at the air-water interface were characterized by measuring the dynamic surface tension (γ) over a time period of 600-seconds. The rate of interfacial tension decay and the final equilibrium tension explain the stability and foaming performance of the barista drinks. The dynamic surface tension profiles characterised through the semi-logarithmic plots, reveal a clear distinction between the kinetic regimes of diffusion (Regime I), adsorption (Regime II), and interfacial relaxation (Regime III) (*Figure 4.9.).*

The comparative analysis of the experimental base samples (S1B-S6B) and the formulated samples (S1F-S6F) showed a significant increase in equilibrium surface tension. All formulated samples demonstrated an immediate decrease in surface tension, indicating that the enzymatic treatments successfully produced surface-active peptides capable of rapid interfacial adsorption. Statistical analysis via one-way ANOVA confirmed that the enzyme specificity significantly influenced the final equilibrium surface tension (p = 0.047), with Samples 5 and 6 reaching the most effective stabilization state at ≈37.4 and 37.8 mN/m respectively.

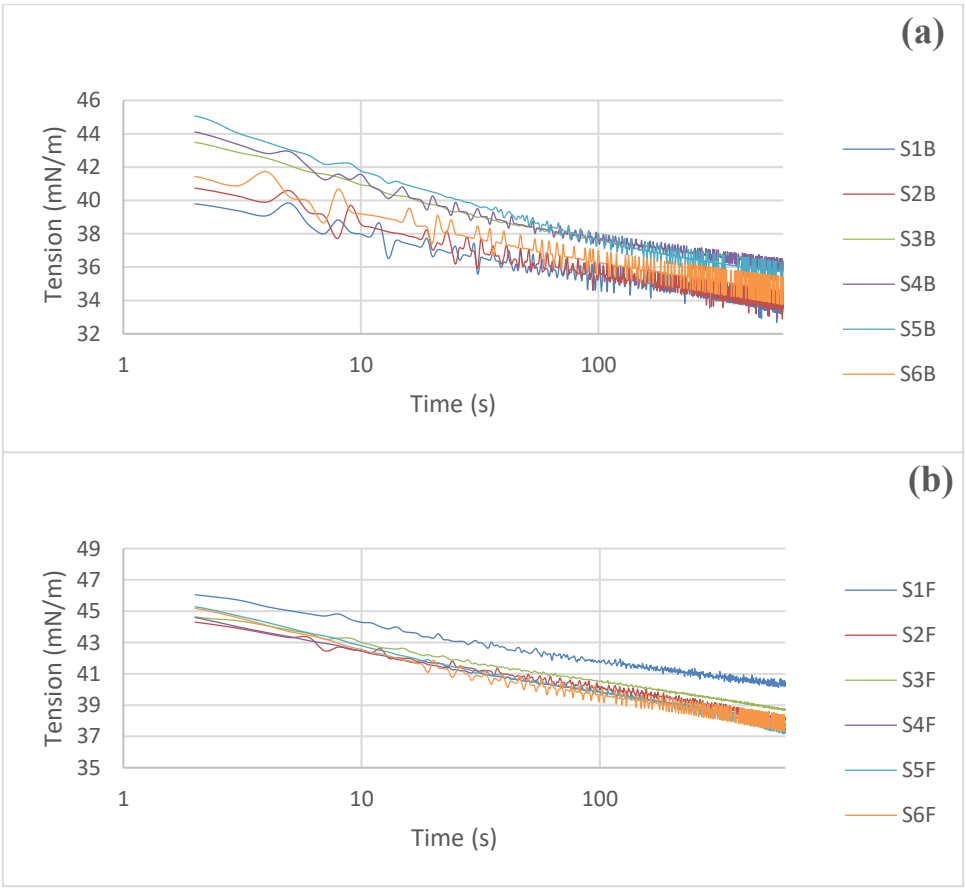

Figure 4.9.: Dynamic surface tension (γ) as a function of logarithmic time (s).

(a) base oat drink samples (b) formulated oat drink samples

The equilibrium surface tension values observed across all formulated sample (≈37.4 to 40.5 mN/m) are notably lower than the typical range for pure globular proteins (47-57 mN/m). As noted by Immonen et al. (2022), these low values are characteristic for oat due to the presence of native polar lipids (phospholipids and glycolipids) that competitively adsorb at the air-water interface.

Sample 5 and 6 exhibited a sustained, linear decay rate in the semi-logarithmic plots through Regimes II and III. This suggests that Protease 4 creates a specific, larger polypeptide fragments, likely similar to the ≈25 kDa fragments identified by (Chen et al., 2023) as ideal stabilizers, that are ideal for stabilization as they are large enough to form a thick protruding layer that provides robust steric stabilization.

Furthermore, as identified by Sethumadhavan et al. (2002), the narrower molecular weight distribution found in the SDS-PAGE for S5 and S6 allowed these peptides to pack neatly into an ordered interfacial structure. This interfacial robustness can be correlated to the functional results, where Samples 5 and 6 demonstrated the highest Foam Stability Index (FSI) (>89%) and highest level of technical reproducibility (variance <1.8) (*Figure 4.10*)

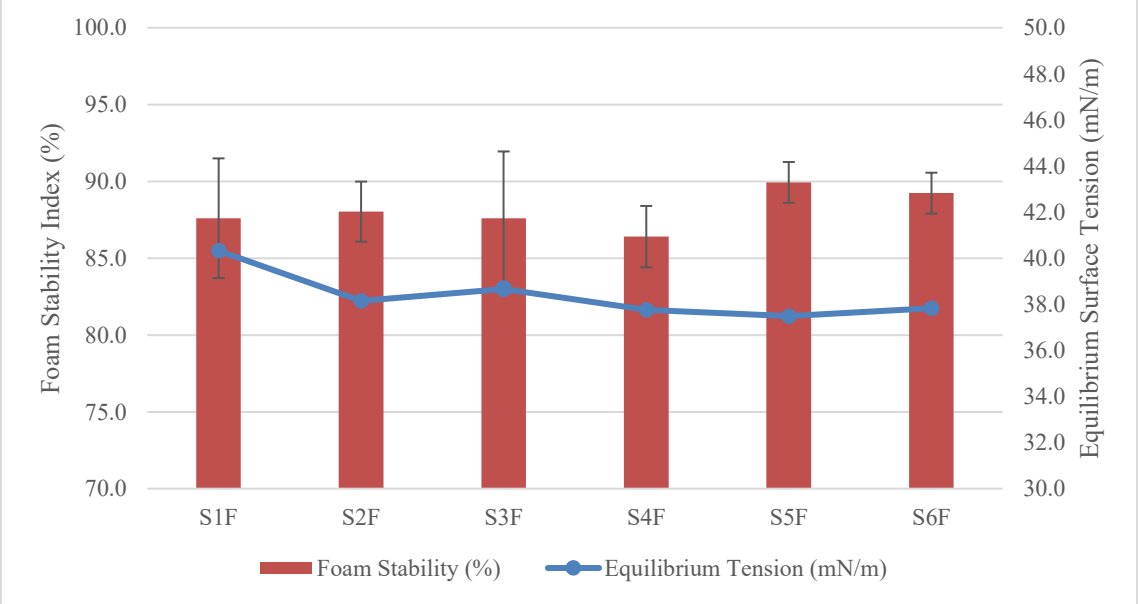

Figure 4.10.: Relationship between equilibrium interfacial tension at t = 600s and the Foam Stability Index (FSI). Bars represent mean FSI (%) ± SD (n = 3); the blue line tracks the mean equilibrium surface tension (mN/m).

Although, Sample 1 achieved the highest protein solubility and a refined physical emulsion (smallest PSD mean diameter), it exhibited the highest formulated surface tension (≈40.5 mN/m). This behaviour is attributed to the high molecular dispersity of the fragments seen as a continuous vertical smear in the SDS-PAGE. Sethumadhavan et al (2002) established that

polydispersity weakens particle layering within thin films and result in foam reduction. This suggests that the lack of structural heterogeneity in Sample 1, inhibited the development of the viscoelastic gel-like network necessary for strong foam stabilization, as evidenced by the lower FSI (≈87.6%) and higher variance (±3.89). Sample 2 depicts the failure of excessive hydrolysis mentioned by Chen et al. (2023). The disappearance of 12S globulin bands in the SDS-PAGE of Sample 2 indicates that Protease 2 achieved extensive cleavage into small peptides. Chen et.al highlight that although these fragments are surface-active, such short fragments can fail to provide the repulsive interaction energy required to keep droplets or bubbles intact. This explains the rapid reach of high surface tension in Sample 2 and its lower FSI. As supported by Zhang et al. (2017), these tiny peptides likely exposed the buried hydrophobic residues, leading to peptide-peptide aggregation and the large 100 μm droplets observed in the PSD resulting in a weak, high-tension interfacial film that resulted in lesser foam stability (FSI=≈88%).

Furthermore, Sample 4 provides evidence that electrostatic repulsion alone is insufficient. While it reached a zeta potential of ≈ −40 mV (matching commercial benchmarks), it showed the lowest FSI (86.4%). This confirms that without structural modification of large, rigid globular proteins into flexible polypeptides, which is essential for developing interfacial network, the negative charge cannot compensate for a lack of cohesive film formation at the air-water interface. Finally, the control Sample 3 validates that starch liquefaction alone cannot replace proteolysis as the native, intact globulins were too rigid to populate the interface effectively. Ultimately, the synergy between high electrostatic charge (≈ -40 mV) and the formation of a viscoelastic film through limited hydrolysis (Regime III relaxation) proves that the Protease 4 formulated drink successfully replicates the stabilization mechanisms of industrial-standard barista milks.

Nevertheless, when evaluated against the practical acceptance criteria used by the industrial partner, the FSI of Sample 1 remained satisfactory, as it exceeded the internal threshold (>85%) which is considered acceptable for oat-based barista beverages. Thus, while Protease 4 appears to be effective for maximising foam stability, Protease 1 may still be considered as a viable option in applications where higher protein solubility and acceptable functional performance are prioritized.

4.6 Functional Stability in Hot Acidic Coffee

The performance benchmark for a barista-grade beverage is its ability to withstand the isoelectric shock when exposed to the hot, acidic environment of brewed coffee (pH ≈ 4.7).

Visual assessment of the formulated oat drinks (S1F-S6F) following addition to coffee revealed a high degree of functional stability across all experimental treatments. As seen in the photographs provided in Appendix C, no visible clumping, feathering or protein flocculation was observed in any of the samples, even after 10 minutes of incubation. However, the varying degree of sedimentation observed at the bottom after 10 minutes correlate with the Trimodal PSD, where the larger fraction of insoluble particles and macro-aggregates underwent gravitational settling.

The functional success observed in the coffee stability test can be correlated to the physicochemical results. The absence of flocculation is a direct validation of the electrostatic stabilization achieved via the alkaline jump observed after formulation (Section 4.3.1) and the resulting high ZP (Section 4.3.2). Simultaneously, the visual sedimentation observed serves as the physical confirmation of the Trimodal PSD (Section 4.4). These results suggests that while the formulation standardises the stability of the beverage in acidic conditions, the rate of physical phase separation depends on the specific enzymatic treatment.

4.7 The Structure-Function Relationship

The results of this study shows that the performance of oat drinks in barista applications is determined by a complex interplay between the extent of proteolysis, the resulting molecular weight distribution, and the electrostatic environment. A clear structure-function relationship emerges by integrating these data from rheological, molecular, and physical analyses.

4.7.1 Proteolytic activity and Colloidal Integrity

A primary finding is that the precision of the enzyme activity is as important as the total protein yield. While Sample 1 achieved the highest soluble protein content (Section 4.2.1), its high terminal viscosity is influenced by the entire colloidal matrix. The presence of larger, polydisperse fragments in Sample 1 (confirmed via SDS PAGE) results in a colloidal system with high structural integrity and provides more structure to the beverage. This suggests that the polydisperse fragments provides a synergistic combination of moderate electrostatic repulsion and steric stabilization resulting in improved solubility.

In contrast, Sample 2 represents excessive hydrolysis. As identified in Section 4.2.2, the disappearance of 12S globulin bands indicates that Protease 2 achieved extensive cleavage into small peptides. In such cases, the total hydrolysis of protein into very small peptides exposes buried hydrophobic residue, leading to peptide-peptide interactions through hydrophobic

interactions that cause the resulting fragments to aggregate and sediment during sedimentation (Y. Zhang et al., 2017). This can be seen in the PSD curve (Section 4.4), where the lack of structural integrity required to form a cohesive viscoelastic film around the oil droplets resulted in rapid coalescence and the formation of large 100 μm aggregates.

4.7.2 Molecular Requirements for Foam Stabilization

The functional superiority shown by Samples 5 and 6 in solubility (next to Sample 1) and foaming indicates that Protease 4 performed a limited hydrolysis sufficient to increase the conformational flexibility of the protein allowing it to unfold and adsorb effectively at the interface. This can be correlated with findings of Hu et al. (2025), who stated that improved emulsion stability upon enzymatic hydrolysis is due to the reduction in particle size and increase in apparent viscosity. Higher viscosity seen in Sample 5 and 6, when combined with refined particle size, resulted in reduced droplet mobility and suppressed coalescence kinetics.

Furthermore, as noted by Immonen et al. (2022), the low equilibrium surface tension measured across all samples is due to the native polar lipids that competitively adsorb at the air-water interface. These lipids reach the interface rapidly and more effectively than protein fragments alone. While this facilitates easy foam formation, these lipids can also act as interfacial impurities that affect the protein-protein interaction and interrupt the development of a cohesive viscoelastic network. The superior stability of Sample 5 and 6 suggests that their uniform fragments (identified by Chen et al., 2023 as ideal stabilizers) were able to arrange neatly into an ordered interfacial structure that overcame this lipid interference.

5. Conclusion

The primary aim of this thesis was to establish a rational, structure-function based approach to enzyme selection for the production of barista-grade oat beverages. Native oat 12S globulins possess a compact, hexameric architecture linked by disulfide bonds that inherently limits their solubility and interfacial functionality (McLauchlan et al., 2024). This study successfully demonstrated that specific enzymatic interventions can overcome these structural constraints by modifying the proteins to withstand the isoelectric shock and thermal stresses encountered during coffee application. Formulation of the beverage plays a critical role in stability by shifting the pH of the beverage from ~6.7 to ~7.7 thereby increasing net negative charge (Zeta potential > -30 mV) to prevent curdling in the acidic coffee environment (Vikenborg & Stensson, 2020).

The experimental results showed that the nature of proteolytic modification is one of the primary determinants of foaming performance. Sample 1 (Protease 1) exhibited high proteolytic efficiency and the highest protein solubility (11.04 mg/mL), providing the beverage with structural integrity and viscosity. However, the resulting polydisperse peptide profile, shown by the continuous vertical smear on the SDS-PAGE, led to reduced foam stability. This polydispersity likely weakened the particle layering within the thin liquid films, resulting in higher equilibrium surface tension (~40.5 mN/m) and lower foam stability (Sethumadhavan et al., 2002). In contrast, Sample 5 and 6 (Protease 4) utilised a limited proteolysis that resulted in less polydisperse molecules. This uniform polypeptide profile allowed an efficient interfacial adsorption, creating a cohesive viscoelastic film that achieved superior foam stability index (FSI) values exceeding 89%.

The study also identified the crucial synergy between viscosity, particle size, and emulsion stability. Sample 2 demonstrated the failure of excessive proteolysis, resulting in small peptides that failed to provide sufficient repulsive energy leading to the formation of large 100 μm aggregates. Meanwhile, Sample 5 and 6 maintained higher terminal viscosities (~31–32 cP) and the microstructural analysis confirmed that these samples achieved refined and well dispersed oil droplet populations. According to Hu et al. (2025), this combination of the fine droplet size and increased viscosity collectively suppress coalescence kinetics.

In conclusion, while the enzyme system with Protease 1 showed better quality in terms of solubility, the lowest mean particulate diameter and acceptable FSI according to internal standards, Protease 4 emerged optimal for foaming stability essential for industrial-standard oat

barista drinks. By achieving a less polydisperse protein profile with a more uniform individual droplet dispersion that facilitates interfacial layering and an apparent viscosity driven by amylase activity that enhances mouthfeel and kinetic stability, this research provides a predicable framework for enzyme selection. These findings confirm that while high solubility and electrostatic repulsion is necessary, the formation of robust, viscoelastic film through targeted, limited proteolysis is essential for developing a high-performance, oat drink for barista application.

6. Future work

Future research should focus on bridging the gap between molecular characterization and commercial application by incorporating sensory evaluation to ensure that no off-flavour is introduced to the beverage by the enzymatic treatments. Additionally, employing SDS-PAGE densitometry would allow for a more precise quantification of specific peptide yields and subunit dissociation, while interfacial dilatational rheology would provide the quantitative mechanical proof of film elasticity needed to resist thermal stress.

References

Anderson, O. D. (2014). The spectrum of major seed storage genes and proteins in oats (Avena sativa). *PloS One*, *9*(7), e83569.

Baldursdottir, S. G., Fullerton, M. S., Nielsen, S. H., & Jorgensen, L. (2010). Adsorption of proteins at the oil/water interface-Observation of protein adsorption by interfacial shear stress measurements. *Colloids and Surfaces B: Biointerfaces*, *79*(1), 41–46. https://doi.org/10.1016/j.colsurfb.2010.03.020

Beverung, C. J., Radke, C. J., & Blanch, H. W. (1999). Protein adsorption at the oilrwater interface: characterization of adsorption kinetics by dynamic interfacial tension measurements. In *Biophysical Chemistry* (Vol. 81).

Bhokarikar, S., Gurumoorthi, P., Athmaselvi, K. A., & Pushpadhas, H. A. (2024). Optimization of process variables for the preparation of oat milk using the Box–Behnken response surface model and studying the effect of enzyme hydrolysis on structural and thermal properties of oat starch. *J. Appl. Biol. Biotechnol*, *12*(6), 261–272.

Bocchi, S., Rocchetti, G., Elli, M., Lucini, L., Lim, C. Y., & Morelli, L. (2021). The combined effect of fermentation of lactic acid bacteria and in vitro digestion on metabolomic and oligosaccharide profile of oat beverage. *Food Research International*, *142*. https://doi.org/10.1016/j.foodres.2021.110216

Brückner-Gühmann, M., Kratzsch, A., Sozer, N., & Drusch, S. (2021). Oat protein as plant-derived gelling agent: Properties and potential of modification. *Future Foods*, *4*. https://doi.org/10.1016/j.fufo.2021.100053

Capek, I. (2002). Sterically and electrosterically stabilized emulsion polymerization. Kinetics and preparation. *Advances in Colloid and Interface Science*, *99*(2), 77–162.

Chen, C., Murray, B. S., & Ettelaie, R. (2023). Surface adsorption properties of peptides produced by non-optimum pH pepsinolysis of proteins: A combined experimental and self-consistent-field calculation study. *Journal of Colloid and Interface Science*, *652*, 405–417. https://doi.org/10.1016/j.jcis.2023.08.040

Creusot, N., & Gruppen, H. (2007). Enzyme-induced aggregation and gelation of proteins. In *Biotechnology Advances* (Vol. 25, Number 6, pp. 597–601). https://doi.org/10.1016/j.biotechadv.2007.07.007

Cui, L., Zhao, J., Jia, Q., Tang, J., Zhong, F., Lu, J., & Zhou, S. (2024). A comparative study on stability and flavor of additive-free oat milk obtained by different heat pretreatments (blanching and microwave) of oat kernels. *Journal of Cereal Science*, *120*. https://doi.org/10.1016/j.jcs.2024.104057

De Santis, D., Frisoni, R., Rossi, A., Ferri, S., & Modesti, M. (2025). Valorization of Local Agricultural Byproducts for the Development of Functional Oat-Based Milk Formulations. *Foods*, *14*(8). https://doi.org/10.3390/foods14081436

Denkov, N., Tcholakova, S., & Politova-Brinkova, N. (2020). Physicochemical control of foam properties. In *Current Opinion in Colloid and Interface Science* (Vol. 50). Elsevier Ltd. https://doi.org/10.1016/j.cocis.2020.08.001

Deswal, A., Deora, N. S., & Mishra, H. N. (2014). Optimization of Enzymatic Production Process of Oat Milk Using Response Surface Methodology. *Food and Bioprocess Technology*, *7*(2), 610–618. https://doi.org/10.1007/s11947-013-1144-2

Fainerman, V. B., Leser, M. E., Michel, M., Lucassen-Reynders, E. H., & Miller, R. (2005). Kinetics of the desorption of surfactants and proteins from adsorption layers at the solution/air interface. *Journal of Physical Chemistry B*, *109*(19), 9672–9677. https://doi.org/10.1021/jp050212o

Gil-González, A. B., Sjögren, L. L. E., Bernfur, K., Olsson, O., & Zambrano, J. A. (2024). Genomic identification of expressed globulin storage proteins in oat. *Frontiers in Plant Science*, *15*. https://doi.org/10.3389/fpls.2024.1418658

Hassan, L., Reynoso, M., Xu, C., Al Zahabi, K., Maldonado, R., Nicholson, R. A., Boehm, M. W., Baier, S. K., & Sharma, V. (2024). The bubbly life and death of animal and plant milk foams. *Soft Matter*, *20*(41), 8215–8229. https://doi.org/10.1039/d4sm00518j

Hlady, V., Buijs, J., & Jennissen, H. P. (1999). [26] Methods for studying protein adsorption. In *Methods in enzymology* (Vol. 309, pp. 402–429). Elsevier.

Horita, K., Kameda, T., Suga, H., & Hirano, A. (2025). Molecular mechanism of the interactions between coffee polyphenols and milk proteins. *Food Research International*, *202*. https://doi.org/10.1016/j.foodres.2024.115573

Ibrahim, M., Aav, A., & Jõudu, I. (2022). The potential and limitations for applications of oat proteins in the food industry. *Agronomy Research*, *20*(1), 161–173. https://doi.org/10.15159/AR.22.008

Immonen, M., Chandrakusuma, A., Hokkanen, S., Partanen, R., Mäkelä-Salmi, N., & Myllärinen, P. (2022). The effect of deamidation and lipids on the interfacial and foaming properties of ultrafiltered oat protein concentrates. *LWT*, *169*. https://doi.org/10.1016/j.lwt.2022.114016

Immonen, M., Myllyviita, J., Sontag-Strohm, T., Myllärinen, P., & Nwachukwu, D. (2021). *Oat Protein Concentrates with Improved Solubility Produced by an Enzyme-Aided Ultrafiltration Extraction Method*. https://doi.org/10.3390/foods

Ipsen, R., Otte, J., Sharma, R., Nielsen, A., Hansen, G., & Qvist, K. B. (2001). Effect of limited hydrolysis on the interfacial rheology and foaming properties of b-lactoglobulin A. In *Colloids and Surfaces B: Biointerfaces* (Vol. 21). www.elsevier.nl/locate/colsurfb

Jaeger, S. R., & Giacalone, D. (2021). Barriers to consumption of plant-based beverages: A comparison of product users and non-users on emotional, conceptual, situational, conative and psychographic variables. *Food Research International*, *144*. https://doi.org/10.1016/j.foodres.2021.110363

Janssen, F., Breugelmans, A., Gunes, D. Z., & Wouters, A. G. B. (2025). Relating the foaming properties of oat proteins to their air-water interfacial characteristics and thin film drainage dynamics. *Food Hydrocolloids*, *167*. https://doi.org/10.1016/j.foodhyd.2025.111426

Jeong, J. H., Hong, S. Y., Cho, J. S., Cho, D. H., & Park, E. Y. (2022). Impact of Enzyme Modification on Physicochemical Properties of Oat Flake and Starch. *Starch/Staerke*, *74*(7–8). https://doi.org/10.1002/star.202100292

Jiang, Z. qing, Sontag-Strohm, T., Salovaara, H., Sibakov, J., Kanerva, P., & Loponen, J. (2015). Oat protein solubility and emulsion properties improved by enzymatic deamidation. *Journal of Cereal Science*, *64*, 126–132. https://doi.org/10.1016/j.jcs.2015.04.010

Kayeye, T. N., Penton, A., Ashton, J., Noyes, S., Sunna, A., Wang, Y., & Rodger, A. (2025). Intermolecular Interactions in Plant Based vs. Animal Milks: A Comparative Review. *Sustainable Food Proteins*, *3*(3). https://doi.org/10.1002/sfp2.70028

Klose, C., & Arendt, E. K. (2012). Proteins in Oats; their Synthesis and Changes during Germination: A Review. In *Critical Reviews in Food Science and Nutrition* (Vol. 52, Number 7, pp. 629–639). https://doi.org/10.1080/10408398.2010.504902

Langevin, D. (2025). On the different coalescence mechanisms in foams and in emulsions. In *Advances in Colloid and Interface Science* (Vol. 340). Elsevier B.V. https://doi.org/10.1016/j.cis.2025.103448

Li, R., & Xiong, Y. L. (2021). Sensitivity of oat protein solubility to changing ionic strength and pH. *Journal of Food Science*, *86*(1), 78–85. https://doi.org/10.1111/1750-3841.15544

Li, R., & Xiong, Y. L. (2023). Disulfide cleavage to improve interfacial behavior and emulsification properties of oat protein. *Food Chemistry*, *404*. https://doi.org/10.1016/j.foodchem.2022.134511

Liu, X., Wang, C., Zhang, X., Zhang, G., Zhou, J., & Chen, J. (2022). Application Prospect of Protein-Glutaminase in the Development of Plant-Based Protein Foods. *Foods*, *11*(3). https://doi.org/10.3390/foods11030440

Mäkinen, O. E., Ercili-Cura, D., Poutanen, K., Holopainen-Mantila, U., Lehtinen, P., & Sozer, N. (2024). Protein from oat: structure, processes, functionality, and nutrition. In *Sustainable protein sources* (pp. 121–141). Elsevier.

McLauchlan, J., Tyler, A. I. I., Chakrabarti, B., Orfila, C., & Sarkar, A. (2024). Oat protein: Review of structure-function synergies with other plant proteins. In *Food Hydrocolloids* (Vol. 154). Elsevier B.V. https://doi.org/10.1016/j.foodhyd.2024.110139

Mendonça, A. P. S., dos Reis, K. L., & Barbosa-Tessmann, I. P. (2023). Aspergillus clavatus UEM 04: An efficient producer of glucoamylase and α-amylase able to hydrolyze gelatinized and raw starch. *International Journal of Biological Macromolecules*, *249*. https://doi.org/10.1016/j.ijbiomac.2023.125890

Munekata, P. E. S., Domínguez, R., Budaraju, S., Roselló-Soto, E., Barba, F. J., Mallikarjunan, K., Roohinejad, S., & Lorenzo, J. M. (2020). Effect of innovative food processing technologies on the physicochemical and nutritional properties and quality of non-dairy plant-based

beverages. In *Foods* (Vol. 9, Number 3). MDPI Multidisciplinary Digital Publishing Institute. https://doi.org/10.3390/foods9030288

Murakami, E., Shionoya, T., Komenoi, S., Suzuki, Y., & Sakane, F. (2016). Cloning and characterization of novel testis-Specific diacylglycerol kinase η splice variants 3 and 4. *PLoS ONE*, *11*(9). https://doi.org/10.1371/journal.pone

Napper, D. H. (1977). Steric stabilization. *Journal of Colloid and Interface Science*, *58*(2), 390–407.

Nieto-Nieto, T. V., Wang, Y. X., Ozimek, L., & Chen, L. (2014). Effects of partial hydrolysis on structure and gelling properties of oat globular proteins. *Food Research International*, *55*, 418–425. https://doi.org/10.1016/j.foodres.2013.11.038

Nnanna, I. A., & Gupta, S. V. (1996). *Purification and Partial Characterization of Oat Bran Globulin*. https://pubs.acs.org/sharingguidelines

Pan, X., Fan, F., Ding, J., Li, P., Sun, X., Zhong, L., & Fang, Y. (2022). Altering functional properties of rice protein hydrolysates by covalent conjugation with chlorogenic acid. *Food Chemistry: X*, *14*. https://doi.org/10.1016/j.fochx.2022.100352

Pei, Y., Hinchliffe, B. A., & Minelli, C. (2021). Measurement of the size distribution of multimodal colloidal systems by laser diffraction. *ACS Omega*, *6*(22), 14049–14058. https://doi.org/10.1021/acsomega.1c00411

Penna, M. J., Mijajlovic, M., & Biggs, M. J. (2014). Molecular-level understanding of protein adsorption at the interface between water and a strongly interacting uncharged solid surface. *Journal of the American Chemical Society*, *136*(14), 5323–5331. https://doi.org/10.1021/ja411796e

Peterson, D. M. (1978). Subunit Structure and Composition of Oat Seed Globulin1. In *Plant Physiol* (Vol. 62).

Peterson, D. M., & Brinegar, A. C. (1986). *Oat storage proteins.*

Pynket, I., Janssen, F., Janssis, V., Maeseele, L., Courtin, C. M., & Wouters, A. G. B. (2026). Colloidal state and emulsifying properties of protein isolates from kilned and non-kilned oats. *Current Research in Food Science*, 101313. https://doi.org/10.1016/j.crfs.2026.101313

Rafique, H., Dong, R., Wang, X., Alim, A., Aadil, R. M., Li, L., Zou, L., & Hu, X. (2022). Dietary-Nutraceutical Properties of Oat Protein and Peptides. In *Frontiers in Nutrition* (Vol. 9). Frontiers Media S.A. https://doi.org/10.3389/fnut.2022.950400

Ramsing, R., Santo, R., Kim, B. F., Altema-Johnson, D., Wooden, A., Chang, K. B., Semba, R. D., & Love, D. C. (2023). Dairy and Plant-Based Milks: Implications for Nutrition and Planetary Health. In *Current Environmental Health Reports* (Vol. 10, Number 3, pp. 291–302). Springer Science and Business Media Deutschland GmbH. https://doi.org/10.1007/s40572-023-00400-z

Robert, L. S., Nozzolillo, C., & Altosaar, I. (1985a). Characterization of oat (Avena sativa L.) residual proteins. *Cereal Chem*, *62*(4), 276–279.

Robert, L. S., Nozzolillo, C., & Altosaar, I. (1985b). Homology between rice glutelin and oat 12 S globulin. In *Biochimica et BiophysicaActa* (Vol. 829).

Rostamabadi, H., Karaca, A. C., Deng, L., Colussi, R., Narita, I. M. P., Kaur, K., Aaliya, B., Sunooj, K. V., & Falsafi, S. R. (2022). Oat starch - How physical and chemical modifications affect the physicochemical attributes and digestibility? In *Carbohydrate Polymers* (Vol. 296). Elsevier Ltd. https://doi.org/10.1016/j.carbpol.2022.119931

Rovai, D., Gupta, S., Watson, M., & Drake, M. A. (2025). Extrinsic Attributes That Drive Oat Milk Purchase. *Journal of Food Science*, *90*(6). https://doi.org/10.1111/1750-3841.70329

Saint-Jalmes, A., & Langevin, D. (2002). Time evolution of aqueous foams: drainage and coarsening. In *J. Phys.: Condens. Matter* (Vol. 14).

Sánchez-Velázquez, O. A., Cuevas-Rodríguez, E. O., Mondor, M., Ribéreau, S., Arcand, Y., Mackie, A., & Hernández-Álvarez, A. J. (2021). Impact of in vitro gastrointestinal digestion on peptide profile and bioactivity of cooked and non-cooked oat protein concentrates. *Current Research in Food Science*, *4*, 93–104.

Sarkar Anwesha and Singh, H. (2016). Emulsions and Foams Stabilised by Milk Proteins. In J. A. McSweeney Paul L. H. and O'Mahony (Ed.), *Advanced Dairy Chemistry: Volume 1B: Proteins: Applied Aspects* (pp. 133–153). Springer New York. https://doi.org/10.1007/978-1-4939-2800-2_5

Sethumadhavan, G., Bindal, S., Nikolov, A., & Wasan, D. (2002). Stability of thin liquid films containing polydisperse particles. In *Colloids and Surfaces A: Physicochemical and Engineering Aspects* (Vol. 204). www.elsevier.com/locate/colsurfa

Sharma, S., Shukla, P., Misra, A., & Mishra, P. R. (2014). Interfacial and colloidal properties of emulsified systems: Pharmaceutical and biological perspective. In *Colloid and interface science in pharmaceutical research and development* (pp. 149–172). Elsevier.

Shay, N., Jing, X., Bhandari, B., Dayananda, B., & Prakash, S. (2023). Effect of enzymatic hydrolysis on solubility and surface properties of pea, rice, hemp, and oat proteins: Implication on high protein concentrations. *Food Bioscience*, *53*, 102515.

Shen, P., Ha, S. M. L., Peng, J., Landman, J., & Sagis, L. M. C. (2025). Role of pulse globulins and albumins in air-water interface and foam stabilization. *Food Hydrocolloids*, *160*. https://doi.org/10.1016/j.foodhyd.2024.110792

Shotwell2, M. A., Afonso, C., Davies, E., Chesnut, R. S., & Larkins, B. A. (1988). Molecular Characterization of Oat Seed Globulins1. In *Plant Physiol* (Vol. 87).

Soycan, G., Schär, M. Y., Kristek, A., Boberska, J., Alsharif, S. N. S., Corona, G., Shewry, P. R., & Spencer, J. P. E. (2019). Composition and content of phenolic acids and avenanthramides in commercial oat products: Are oats an important polyphenol source for consumers? *Food Chemistry: X*, *3*. https://doi.org/10.1016/j.fochx.2019.100047

Sridharan, S., Meinders, M. B. J., Bitter, J. H., & Nikiforidis, C. V. (2020). On the Emulsifying Properties of Self-Assembled Pea Protein Particles. *Langmuir*, *36*(41), 12221–12229. https://doi.org/10.1021/acs.langmuir.0c01955

Tarahi, M., Gharagozlou, M., Niakousari, M., & Hedayati, S. (2024). Protein–Chlorogenic Acid Interactions: Mechanisms, Characteristics, and Potential Food Applications. In *Antioxidants* (Vol. 13, Number 7). Multidisciplinary Digital Publishing Institute (MDPI). https://doi.org/10.3390/antiox13070777

Vikenborg, C., & Stensson, F. (2020). *Functionality of oat based food ingredients*.

Wagner, J. R., Sorgentini, D. A., & Anon, M. C. (2000). Relation between solubility and surface hydrophobicity as an indicator of modifications during preparation processes of commercial and laboratory-prepared soy protein isolates. *Journal of Agricultural and Food Chemistry*, *48*(8), 3159–3165. https://doi.org/10.1021/jf990823b

Wang, J., Wang, T., Yu, G., Li, X., Liu, H., Liu, T., & Zhu, J. (2022). Effect of enzymatic hydrolysis on the physicochemical and emulsification properties of rice bran albumin and globulin fractions. *LWT*, *156*. https://doi.org/10.1016/j.lwt.2021.113005

Wang, X., Ye, A., Dave, A., & Singh, H. (2022). Structural changes in oat milk and an oat milk–bovine skim milk blend during dynamic in vitro gastric digestion. *Food Hydrocolloids*, *124*. https://doi.org/10.1016/j.foodhyd.2021.107311

Wouters, A. G. B., Rombouts, I., Fierens, E., Brijs, K., & Delcour, J. A. (2016). Relevance of the Functional Properties of Enzymatic Plant Protein Hydrolysates in Food Systems. In *Comprehensive Reviews in Food Science and Food Safety* (Vol. 15, Number 4, pp. 786–800). Blackwell Publishing Inc. https://doi.org/10.1111/1541-4337.12209

Yano, Y. F., Arakawa, E., Voegeli, W., Kamezawa, C., & Matsushita, T. (2018). Initial Conformation of Adsorbed Proteins at an Air-Water Interface. *Journal of Physical Chemistry B*, *122*(17), 4662–4666. https://doi.org/10.1021/acs.jpcb.8b01039

Yazghur, P., Mikhailovskaya, A., Forel, E., Schneider, M., Rio, E., Salonen, A., & Langevin, D. (2018). Coarsening of aqueous foams. microgravity experiments. *69th International Astronautical Congress (IAC)*.

Zafeiri, I., Smith, P., Norton, I. T., & Spyropoulos, F. (2017). Fabrication, characterisation and stability of oil-in-water emulsions stabilised by solid lipid particles: The role of particle characteristics and emulsion microstructure upon Pickering functionality. *Food and Function*, *8*(7), 2583–2591. https://doi.org/10.1039/c7fo00559h

Zakidou, P., Varka, E. M., & Paraskevopoulou, A. (2022). Foaming properties and sensory acceptance of plant-based beverages as alternatives in the preparation of cappuccino style beverages. *International Journal of Gastronomy and Food Science*, *30*. https://doi.org/10.1016/j.ijgfs.2022.100623

Zhan, X., Zhang, J., Xing, J., Xu, J., Ouyang, D., Wang, L., Wan, Y., & Luo, X. (2025). Synergistic Amylase and Debranching Enzyme Catalysis to Improve the Stability of Oat Milk. *Foods*, *14*(7). https://doi.org/10.3390/foods14071271

Zhang, H., Zhao, X., Chen, X., & Xu, X. (2022). Thoroughly review the recent progresses in improving O/W interfacial properties of proteins through various strategies. *Frontiers in Nutrition*, *9*, 1043809.

zhang, M., Fan, L., Liu, Y., Huang, S., & Li, J. (2022). Effects of proteins on emulsion stability: The role of proteins at the oil–water interface. In *Food Chemistry* (Vol. 397). Elsevier Ltd. https://doi.org/10.1016/j.foodchem.2022.133726

Zhang, Y., Zhou, F., Zhao, M., Ning, Z., Sun-Waterhouse, D., & Sun, B. (2017). Soy peptide aggregates formed during hydrolysis reduced protein extraction without decreasing their nutritional value. *Food and Function*, *8*(12), 4384–4395. https://doi.org/10.1039/C7FO00812K

Zhao, Y., Mine, Y., & Ma, C. Y. (2004). Study of Thermal Aggregation of Oat Globulin by Laser Light Scattering. *Journal of Agricultural and Food Chemistry*, *52*(10), 3089–3096. https://doi.org/10.1021/jf030735y

Appendixes

Appendix A: Relative Viscosity (% of initial)

Table A1.: Relative viscosity (%) of oat drink samples across enzymatic hydrolysis duration.

Time	Sample 1	Sample 2	Sample 3	Sample 4	Sample 5	Sample 6
15	100	100	100	100	100	100
30	73.33	73.5	68.1	74.9	74.0	78.5
45	66.1	63.3	58.0	63.0	65.4	65.5
60	61.8	54.2	53.9	54.8	57.5	59.1

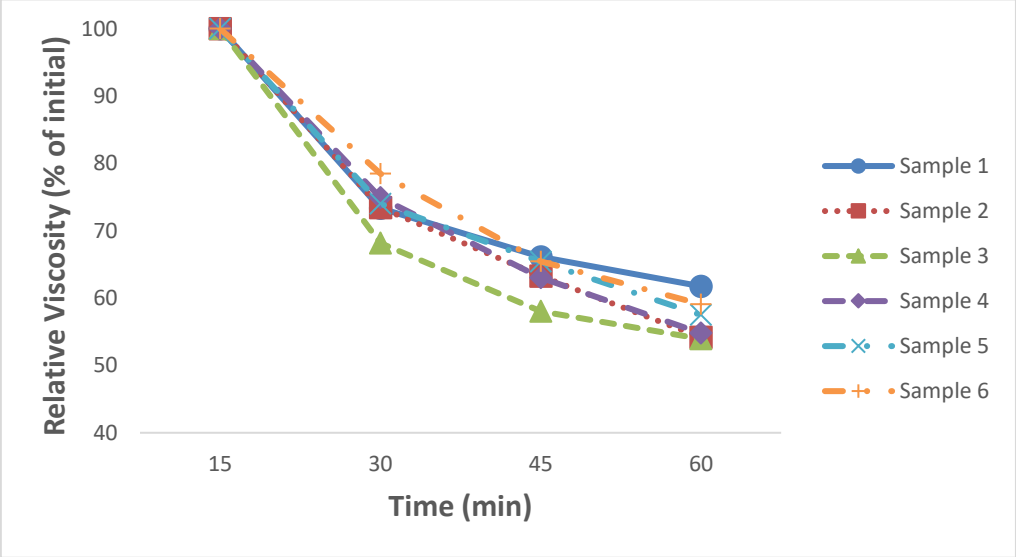

Figure A1.: *Normalized liquefaction efficiency represented as relative viscosity (% of initial) across 60 minutes of enzymatic hydrolysis.*

Appendix B: Microstructural Analysis

Table B1.: Microscopic assessment of formulated oat beverages (middle layer) (10x magnification).

Sample ID	Microscopic Image	Interpretation
Sample 1	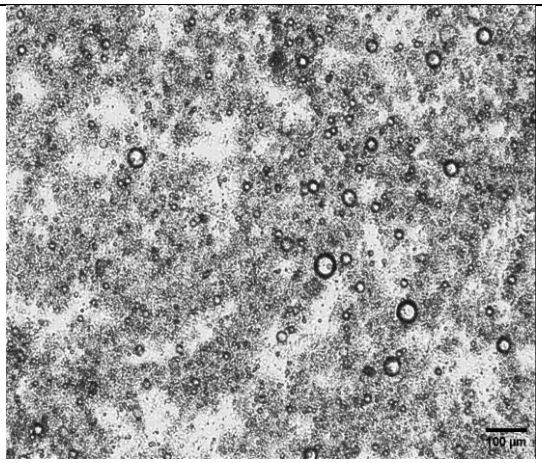	Exhibits a high density of well-dispersed spherical oil droplets confirming the presence of the polydisperse peptides
Sample 2	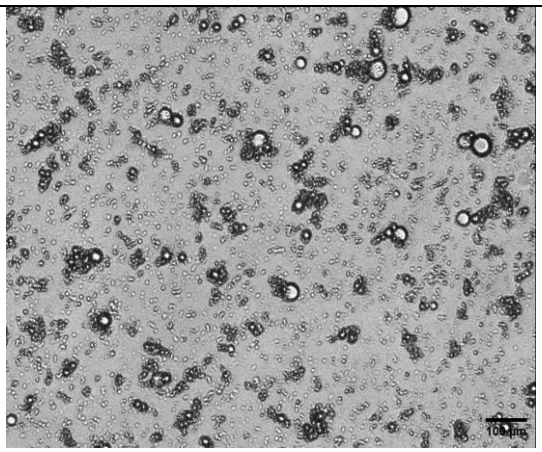	Characterised by large, irregular dark masses and coalesced oil clusters
Sample 3	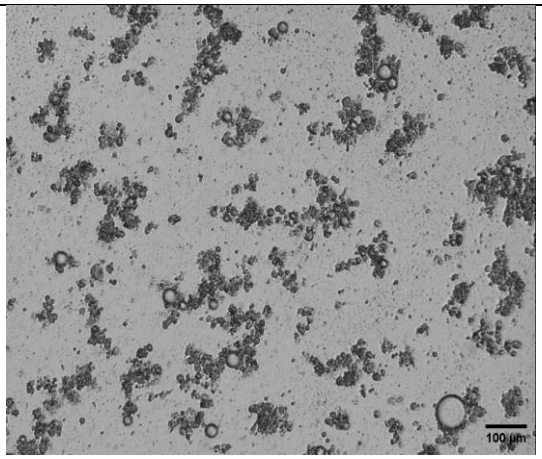	Dominated by clusters of unhydrolyzed native protein-starch complexes.

Sample ID	Microscopic Image	Interpretation
Sample 4	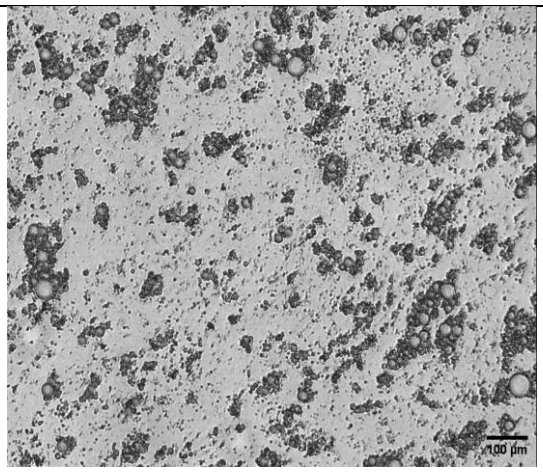	Shows a mix of small droplets and large, irregular aggregates
Sample 5	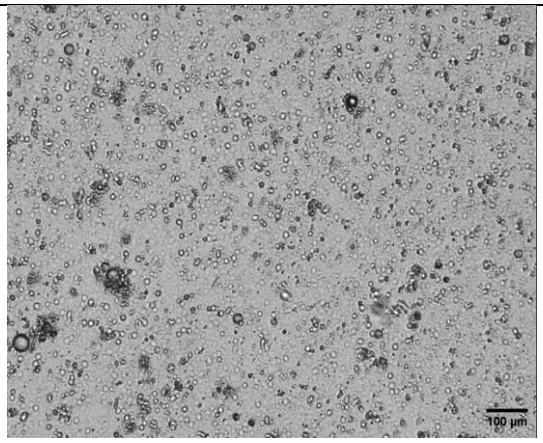	Displays a field of fine droplets but with persistent irregular flocs.
Sample 6	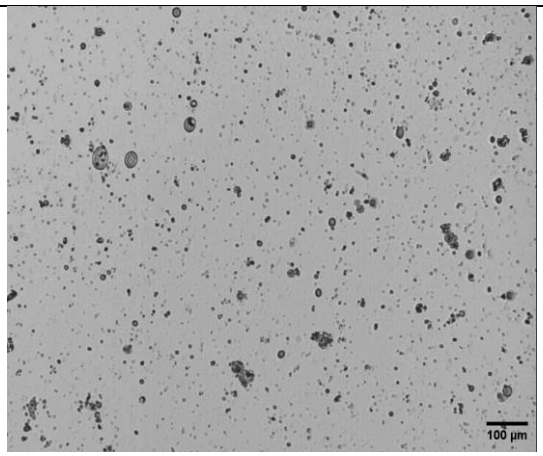	Exhibits a uniform dispersion of individual droplets with minimal macro-aggregates

Appendix C: Coffee Stability

Table C1.: Pictures of Coffee Stability test on six experimental formulated oat beverages

Sample ID	5 minutes	10 minutes
Sample 1	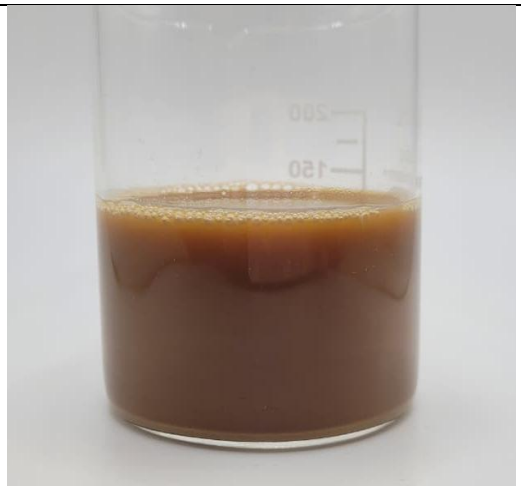	
Sample 2	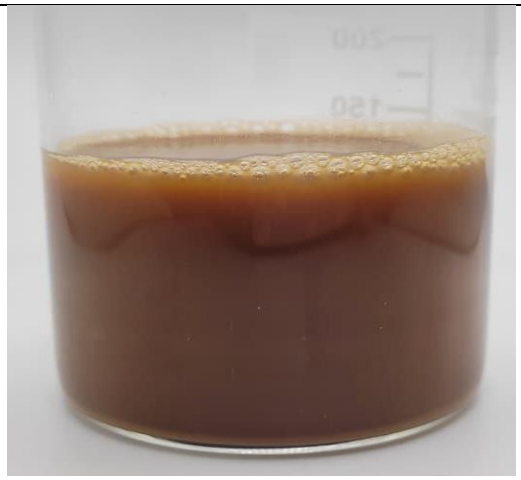	
Sample 3		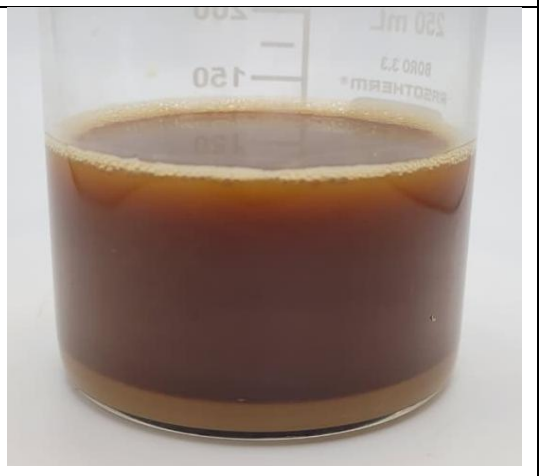

Sample ID	5 minutes	10 minutes
Sample 4	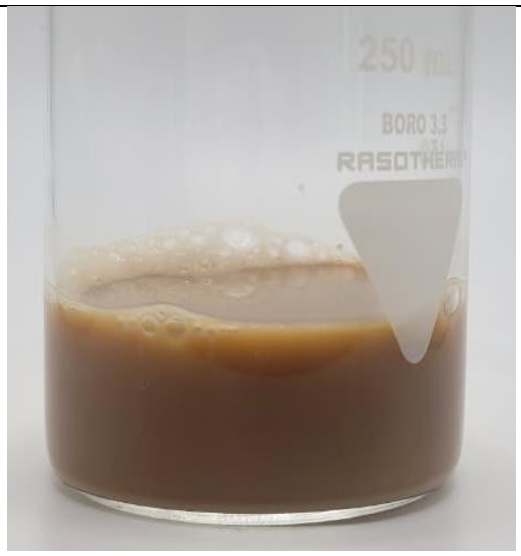	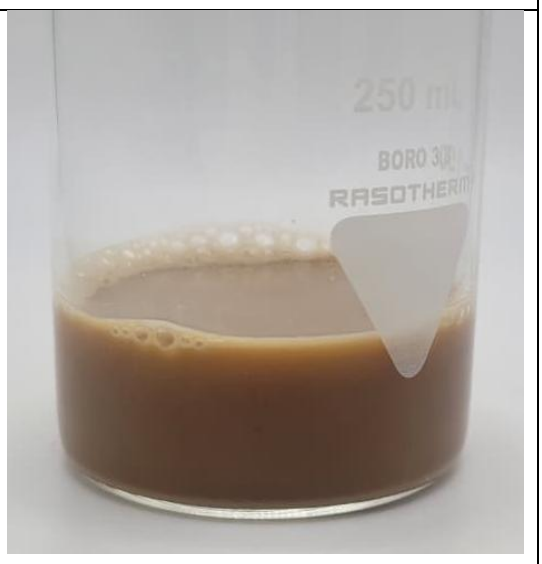
Sample 5	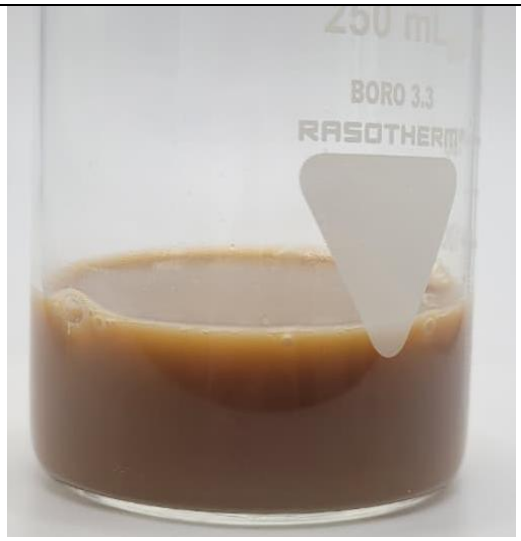	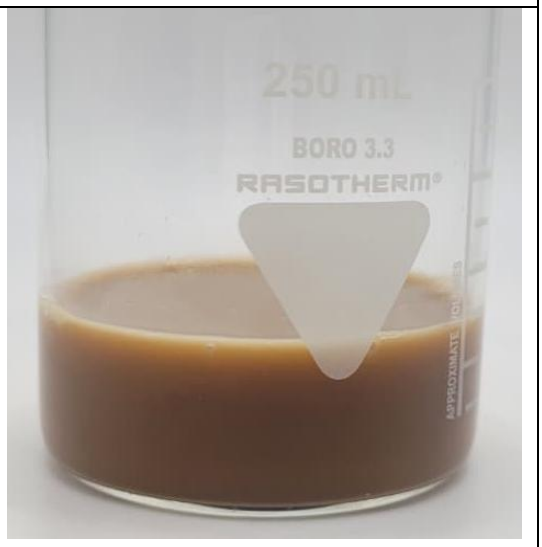
Sample 6	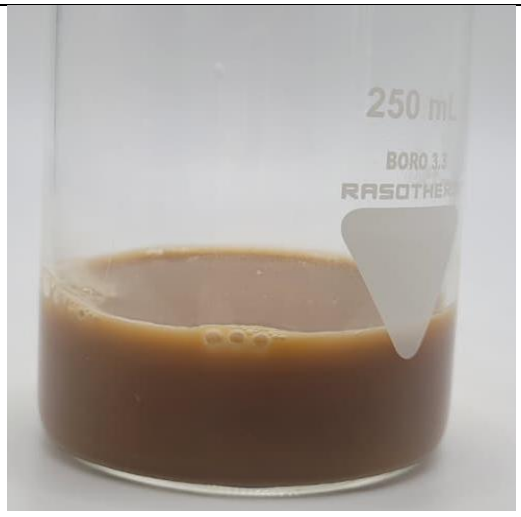	

Appendix D: Statistical Data

Table D1: One-way ANOVA of terminal viscosity

SUMMARY

Groups	*Count*	*Sum*	*Average*	*Variance*
Sample 1	3	88	29.33333	3.583333
Sample 2	3	74.5	24.83333	1.083333
Sample 3	3	85.5	28.5	1.75
Sample 4	3	83	27.66667	2.583333
Sample 5	3	94	31.33333	1.083333
Sample 6	3	97.5	32.5	6.75

ANOVA

Source of Variation	*SS*	*df*	*MS*	*F*	*P-value*	*F crit*
Between Groups	111.5694	5	22.31389	7.953465	0.001633	3.105875
Within Groups	33.66667	12	2.805556			
Total	145.2361	17				

Table D2: Two-factor ANOVA on soluble protein concentration in base and formulated samples

SUMMARY	S1	S2	S3	S4S	S5	S6	Total
Base							
Count	3	3	3	3	3	3	18
Sum	33.13	22.72	23.73	20.57	23.21	24.03	147.39
	11.0433	7.57333		6.85666	7.73666666		8.18833
Average	3	3	7.91	7	7	8.01	3
	0.67573	0.23003		2.79743	1.16603333		2.75080
Variance	3	3	0.1497	3	3	2.4391	3
Formulated							
Count	3	3	3	3	3	3	18
Sum	37.16	33.73	30.89	30.39	33.66	33.72	199.55
	12.3866	11.2433	10.2966				11.0861
Average	7	3	7	10.13	11.22	11.24	1
	0.41643	4.90843	3.65903				3.13051
Variance	3	3	3	2.8147	3.5644	6.3037	9
Total							
Count	6	6	6	6	6	6	
Sum	70.29	56.45	54.62	50.96	56.87	57.75	
		9.40833	9.10333	8.49333	9.47833333		
Average	11.715	3	3	3	3	9.625	

Variance	0.97823	6.096057	3.232347	5.459267	5.532256667	6.62699

ANOVA

Source of Variation	*SS*	*df*	*MS*	*F*	*P-value*	*F crit*
Sample	75.57404	1	75.57404	31.13809	9.64741E-06	4.259677
Columns	35.93079	5	7.186158	2.960847	0.032060456	2.620654
Interaction	5.802222	5	1.160444	0.478127	0.788943423	2.620654
Within	58.24947	24	2.427061			
Total	175.5565	35				

Table D3: Two-factor ANOVA on pH of Base and Formulated Samples

SUMMARY	Base	Formulated	Total
S1			
Count	3	3	6
Sum	19.91	22.82	42.73
Average	6.636667	7.606667	7.121667
Variance	0.003233	0.010233	0.287657
S2			
Count	3	3	6
Sum	20.19	23.33	43.52
Average	6.73	7.776667	7.253333
Variance	0.0147	0.009433	0.338307
S3			
Count	3	3	6
Sum	20.83	23.2	44.03
Average	6.943333	7.733333	7.338333
Variance	0.018633	0.001733	0.195377
S4			
Count	3	3	6
Sum	20.44	23.29	43.73
Average	6.813333	7.763333	7.288333
Variance	0.003033	0.003733	0.273457
S5			

Count	3	3	6
Sum	20.43	23.42	43.85
Average	6.81	7.806667	7.308333
Variance	0.0613	0.005633	0.324777

S6			
Count	3	3	6
Sum	20.09	23.1	43.19
Average	6.696667	7.7	7.198333
Variance	0.004433	0.0063	0.306297

Total		
Count	18	18
Sum	121.89	139.16
Average	6.771667	7.731111
Variance	0.022674	0.008822

ANOVA

Source of Variation	*SS*	*df*	*MS*	*F*	*P-value*	*F crit*
Sample	0.190881	5	0.038176	3.217088	0.023098	2.620654
Columns	8.284803	1	8.284803	698.1575	2.97E-19	4.259677
Interaction	0.059747	5	0.011949	1.006976	0.435057	2.620654
Within	0.2848	24	0.011867			
Total	8.820231	35				

Table D4: Two-factor ANOVA on Zeta-potential of Base and Formulated Samples

SUMMARY	Base	Formulated	Total
Sample 1			
Count	3	3	6
Sum	-92.1	-98.7	-190.8
Average	-30.7	-32.9	-31.8
Variance	0.39	1.33	2.14
Sample 2			
Count	3	3	6
Sum	-83.5	-98.8	-182.3
Average	-27.8333	-32.9333	-30.3833
Variance	9.503333	0.363333	11.74967
Sample 3			
Count	3	3	6
Sum	-116.1	-115.4	-231.5

Average	-38.7	-38.4667	-38.5833
Variance	28.12	6.843333	14.00167

Sample 4			
Count	3	3	6
Sum	-100.1	-122.7	-222.8
Average	-33.3667	-40.9	-37.1333
Variance	2.613333	40.99	34.46667

Sample 5			
Count	3	3	6
Sum	-109.9	-119.5	-229.4
Average	-36.6333	-39.8333	-38.2333
Variance	17.60333	2.623333	11.16267

Sample 6			
Count	3	3	6
Sum	-118.2	-123.8	-242
Average	-39.4	-41.2667	-40.3333
Variance	15.19	31.86333	19.86667

Total		
Count	18	18
Sum	-619.9	-678.9
Average	-34.4389	-37.7167
Variance	27.40487	22.91794

ANOVA

Source of Variation	*SS*	*df*	*MS*	*F*	*P-value*	*F crit*
Sample	485.2456	5	97.04911	7.397349	0.000254	2.620654
Columns	96.69444	1	96.69444	7.370315	0.012088	4.259677
Interaction	55.37556	5	11.07511	0.844175	0.531936	2.620654
Within	314.8667	24	13.11944			
Total	952.1822	35				

Table D5: One-way ANOVA on PSD of the 6 experimental base formulated samples

SUMMARY

Groups	*Count*	*Sum*	*Average*	*Variance*
S1	3	73.587	24.529	0.086932
S2	3	153.25	51.08333	18.32399
S3	3	119.042	39.68067	3.302804
S4	3	121.294	40.43133	61.2566
S5	3	122.966	40.98867	51.23795

S6	3	120.898	40.29933	0.12756

ANOVA

Source of Variation	*SS*	*df*	*MS*	*F*	*P-value*	*F crit*
Between Groups	1086.179	5	217.2357	9.702655	0.000675	3.105875
Within Groups	268.6717	12	22.38931			
Total	1354.85	17				

Table D6: One-way ANOVA on equilibrium surface tension of the six experimental formulated samples

SUMMARY

Groups	*Count*	*Sum*	*Average*	*Variance*
S1	2	80.28	40.14	0.254422
S2	2	75.89333	37.94667	0.554756
S3	2	77.63	38.815	0.16245
S4	2	76.87667	38.43833	0.04805
S5	2	74.79667	37.39833	0.001606
S6	2	74.97333	37.48667	1.7672

ANOVA

Source of Variation	*SS*	*df*	*MS*	*F*	*P-value*	*F crit*
Between Groups	10.47843	5	2.095686	4.509303	0.047151	4.387374
Within Groups	2.788483	6	0.464747			
Total	13.26691	11				

Appendix F: Oat Drink Stability Study

Table F1: Images of the three layers formed after keeping the oat drink undisturbed overnight

Sample ID	Stability Study Images
Sample 1	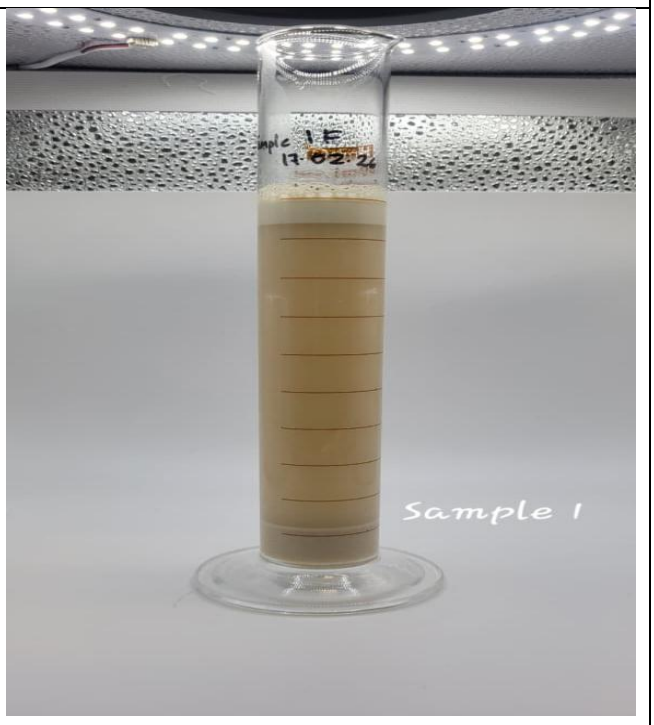
Sample 2	

Sample ID	Stability Study Images
Sample 3	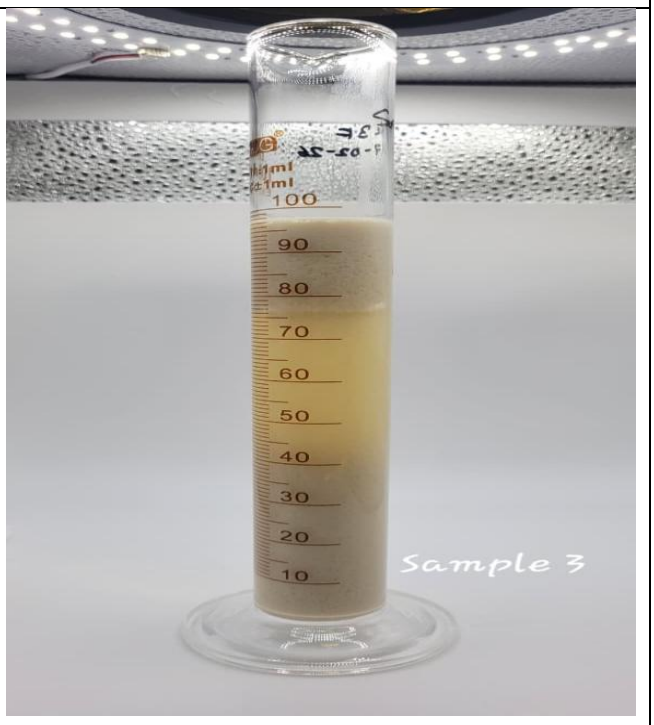
Sample 4	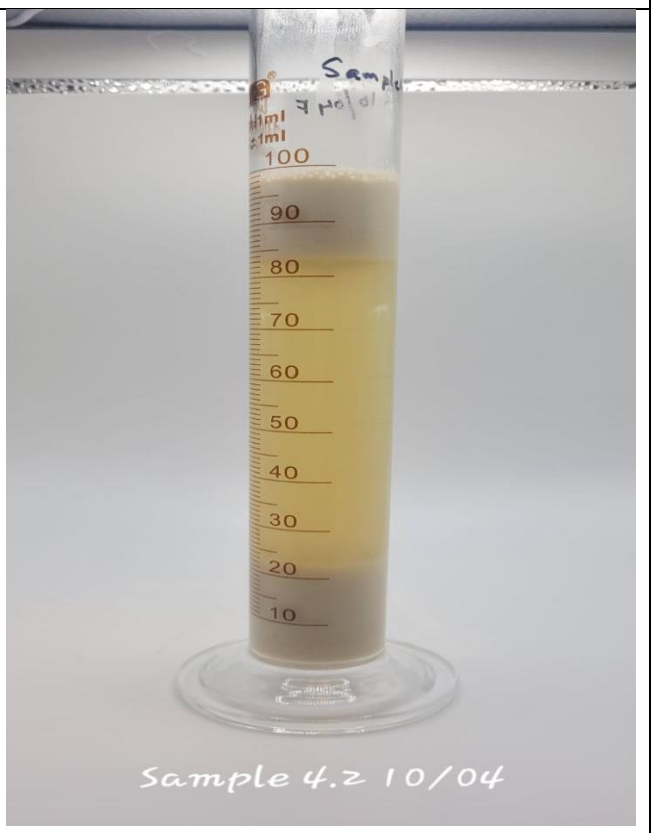

Sample ID	Stability Study Images
Sample 5	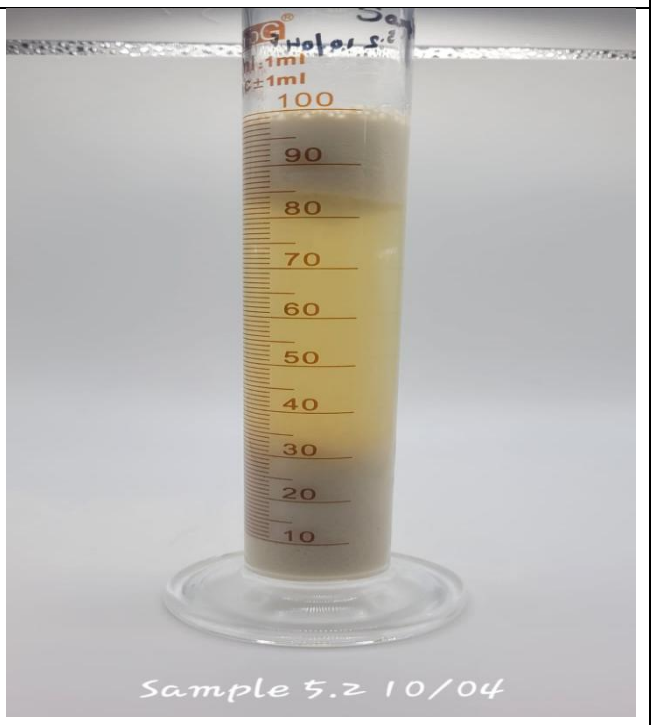
Sample 6